Aerodynamic Prediction for Low Reynolds Numbers

Daniel L. Shaffer and Michael S. Turner

Advisor Dr. Robert C. Nelson

Department of Aerospace and Mechanical Engineering
University of Notre Dame

April 28, 2010

Abstract

A Reynolds number is a characteristic quantity of any body moving through a fluid and represents the ratio of the inertial forces to the viscous forces experienced in motion. The Reynolds number is a fundamental quantity that permeates the study of aerodynamics and functions as a scaling factor for all aerodynamic calculations. Modern aircraft design has focused primarily on large aircraft which, due to their greater sizes and velocities, have relatively large Reynolds numbers. As unmanned aerial vehicles become more viable, however, the study of low Reynolds number air flows has become more prevalent. While the process for analyzing and predicting the aerodynamic characteristics in low Reynolds number aircraft is comparable to that in large scale aircraft, the results are significantly different. With the intent of simplifying the design process of radio controlled aircraft by providing a basis for predicting the aerodynamic characteristics, a database which compares aerodynamic specifications is developed. Using information from a variety of radio controlled aircraft designs, the database allows for the prediction of trends in these specifications. Additionally, the performance characteristics, drag, and lift are assessed for these designs, allowing for additional reference in predicting the characteristics of a proposed aircraft design. Equations and theories which have traditionally been applied to full-scale aircraft are adapted for use with low Reynolds number vehicles to aid in establishing a method for predicting the aerodynamics of these small airplanes.

Section 1

Precedent Data Acquisition

During the initial stages of aircraft design, the best method for predicting the aerodynamic characteristics of the new aircraft is to study the aerodynamic and performance parameters of similar precedent designs. Using past data provides a starting point; from this point the design can be refined and adapted to the specific design constraints which are presented in the current design effort. Even large aerospace companies frequently use data from past designs as an initial reference for new aircraft. In this manner, the starting point of the aerodynamic and performance analysis of low Reynolds number vehicles will be the data available for current radio-controlled aircraft.

Because of the countless radio-controlled aircraft designs currently available, there exists a variety of aircraft styles and sizes which can be analyzed. However, the data which is available for each aircraft is limited. The basic aircraft dimensions and specifications, including wingspan, fuselage length, and weight, are typically given, but the performance characteristics are generally not given for radio-controlled aircraft. In addition, the detailed dimensions, including tire diameter and horizontal tail width, are not specified. While the performance characteristics can be estimated through a performance analysis, the unspecified dimensions must be estimated from photos of each aircraft design. By using reference photos, the relative size between a known dimension and an unknown dimension can be established. Using this relationship, the unknown dimension can be approximated with significant accuracy.

To be an accurate predictor of aerodynamics, the precedent aircraft must have similar design qualities and specifications when compared to the proposed aircraft. This is a fundamental component of analyzing low Reynolds aircraft separately from full-scale aircraft: the data from full-scale aircraft cannot be effectively used to predict the aerodynamics of a low Reynolds number aircraft. The radio-controlled aircraft considered for this analysis are all powered by an electric motor. Additionally, they are all constructed in a simple manner, consisting of plastic film covering over a simple wood frame. The fuselage must have a three-

dimensional shape which can be approximated by a cylinder with rounded ends. The final constraints are that the precedent aircraft should not have flaps (or other high-lift devices), and must have fixed landing gear. Both high-wing and low-wing aircraft are considered for this analysis.

In order to fully analyze the power plant and drag characteristics of each aircraft in preparation for estimating the performance parameters, the dimensions of all major components of the aircraft are needed, including the wing, fuselage, horizontal and vertical tail, tires and landing hear strut, and the propeller. Additionally, the maximum current, maximum voltage, and maximum rate of revolution for the motor are needed.

The data which is acquired for each aircraft will be the basis of the remainder of the drag and performance analysis. Using a relatively limited and simple data set, the application of standard aerodynamic and performance can lead to substantial aerodynamic calculations with considerable accuracy. This will be the subject matter of the next three sections.

Section 2

Power Plant and Propeller Analysis

The analysis of aircraft performance commences with an investigation of motor specifications. As the source of an aircraft's thrust, a power plant must transmit sufficient power to the propeller to overcome drag and allow for the generation of lift. The motor's power is calculated as electrical work per unit time and is transmitted to the propeller as mechanical work per unit time. For the electric motors considered here, a motor's output power is a function of voltage and current and is subject to shaft output efficiency. Power is calculated as follows

$$P = VI \qquad\qquad (2.1)$$

where V is voltage in Volts, I is current in Amps, and sec denotes the one second time interval. The power P is measured in Watts. Sample calculations are shown for the Turborix D2836 Brushless motor produced by AirLandSea Hobbies. The motor's specifications state the maximum voltage as 11.1 V and the load current to be 28A. The power is calculated as

$$P = 11.1V \cdot 28A = 310.8\ W \qquad\qquad (2.2)$$

The calculated power of 310.8 W is slightly below the motor's specified maximum power of 355 W.

Alternatively, the voltage of many motors is reported relative to the output shaft's revolution rate (the rotations per minute) with units of volts per rotations per minute. This rpm/V specification is dependent upon the size of the motor: the shaft's revolution rate increases less per unit of applied electromotive force (voltage) in larger motors. This is primarily due to greater moment of inertia of the output shaft (and the propeller) associated with larger motors (and propellers). The relationship between voltage and revolution rate is linear, meaning that the relationship between revolution rate and power is also linear, and can be used to calculate power:

$$P = \left[f \left(\frac{V}{f} \right) I \right] \qquad (2.3)$$

where f denotes the frequency (rate of revolution) of the output shaft, which is usually reported in rpm for aircraft motors. Using this relationship, the maximum revolution rate corresponds to the maximum voltage, which, in turn, corresponds to the maximum power. While the validity of this equation is readily apparent because the frequency terms cancel out, it is useful for radio controlled aircraft analysis because the voltage is commonly given in terms of the rpm.

Again using the D2386 motor specifications, the manufacturer's specified rotational rate is 12,600 rotations per minute. Additionally the specified ratio of rpm to voltage is 1000 rpm/V. To calculate power, however, the ratio of voltage to rpm is needed, which is simply the reciprocal of this value, or 0.001 Volts per rpm. Inserting values yields

$$P = \left[(12600 \; rpm) \left(\frac{V}{1000 \; rpm} \right) (28A) \right] = 352.8 \; W \qquad (2.4)$$

This value of 352.8 Watts is within the margin of error of the motor's published power of 355 Watts.

The final consideration in calculating the output power is the motor's efficiency. The input voltage and the current used by the motor must be multiplied by an efficiency factor in order to determine the output shaft power. Most radio controlled aircraft motors have efficiencies of 75% to 90%, where the energy loss is due to heat production, noise, and vibrations. Additionally, motors which operate at higher powers have greater efficiencies; Figure 2.1 displays the approximate relationship between motor input power (before it is subjected to an efficiency factor) and the motor efficiency. Above input powers of 1200 W, motors consistently exhibit efficiencies of about 92%.

Once a motor's shaft power has been established, this value is the basis of calculating propeller and thrust characteristics. The motor's output affects the propeller's performance which, in turn, dictates the amount of thrust produced. With the ultimate objective of analyzing the aircraft's overall aerodynamic performance, the propeller is the key intermediary in transforming the motor's electrical work into the mechanical work which propels an aircraft. The mechanical work generated by a motor and propeller assembly is simply the force (produced by
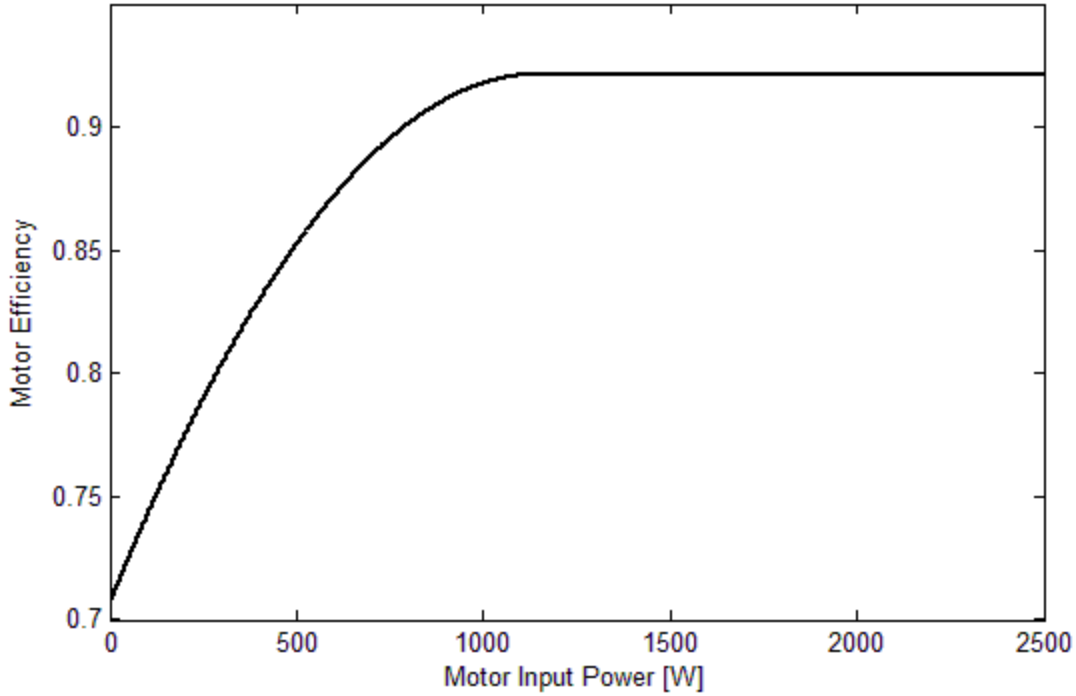
Figure 2.1: Approximate Relationship Between Motor Input Power and Motor Efficiency.

thrust) multiplied by the component of the displacement in the direction of that force. For an aircraft which produces thrust in the direction of flight (the direction of displacement),

$$W = \int_{x_1}^{x_2} T \, dx \tag{2.5}$$

$$dW = T \, dx \tag{2.6}$$

in which T is the total thrust force, x is the displacement, and x_1 and x_2, the limits of integration, are the initial and final positions. These can be reported in any units, as long as those units are consistent. Because instantaneous power is the time rate of change of work, Equation 2.5 can be altered to describe the power which is produced by the thrust force:

$$P = \lim_{\Delta t \to 0} \frac{\Delta W}{\Delta t} = \frac{dW}{dt} = T \frac{dx}{dt} = T\dot{x} = Tv \tag{2.7}$$

where $\dot{x}$ and v both denote the propeller velocity (the velocity of air flowing through the propeller without considering the effects of drag). Equation 2.1, the power of the motor, and

7

Equation 2.7, the power provided by the propeller's thrust, are clearly linked to each other. However, efficiency acts as an intervening element. The motor's power is subjected to an efficiency factor as the propeller converts the energy into a thrust force. Therefore, the relationship between the power produced by the motor and the power derived from the propeller can be expressed as

$$P_{prop} = \eta_{prop}\,\eta_{motor}\,P_{motor} \tag{2.8}$$

$$Tv = \eta_{prop}\,\eta_{motor}\,VI \tag{2.9}$$

where η_{prop} is the propeller efficiency factor and η_{motor} is the motor efficiency factor. While this is the primary relationship between the motor's power and the propeller's power, there are numerous intermediary equations which relate parameters of the motor and propeller to the thrust and efficiency. By using these equations, the manufacturer's motor and propeller specifications can aid in calculating the propeller efficiency and thrust. The first equation defines the advance ratio J of a propeller:

$$J = \frac{v}{nD} \tag{2.10}$$

in which v is the axial (forward) velocity of the propeller in feet per second or meters per second, n is the revolution rate in rotations per second, and D is the diameter of the propeller in feet or meters. Qualitatively, the advance ratio is the axial distance traveled by the propeller (and thus also the aircraft) during one propeller revolution.

The pitch to diameter ratio of propellers is frequently referenced in thrust and performance equations, and is simply the ratio of these two dimensions. The pitch of the propeller is the axial distance traveled by the propeller during one rotation if the propeller were rotating in a solid medium, similar to a screw through wood.

The first equation which incorporates both propeller specifications and performance relates a motor's shaft (output) power to the propeller and motor characteristics:

$$P_s = \eta_{motor}\,VI = C_p \rho n^3 D^5 \tag{2.11}$$

where ρ is the air density. The variable C_p is the motor's power coefficient and is a function of the propeller's advance ratio and the propeller's pitch to diameter ratio. Figure 2.2 displays the relationship between power coefficient and advance ratio for various pitch to diameter ratios. The propeller specifications can also be used to find the total thrust using

$$T = C_t \rho n^2 D^4 \tag{2.12}$$

in which C_t is the thrust coefficient, a function of the propeller advance ratio and pitch to diameter ratio. Figure 2.3 shows the relationship between the thrust coefficient and the advance ratio for varying pitch to diameter ratios.

Finally, the propeller efficiency must be considered. The efficiency represents the ratio of thrust power to motor power, and is calculated using the relationship

$$\eta_{prop} = \frac{C_t J}{C_p} \tag{2.13}$$

Of particular importance is the observation that all of these equations are components of the primary power formula, Equation 2.9. This can be proven by simply substituting Equations 2.10 through 2.13 into Equation 2.9 and confirming the validity of the result:

$$Tv = \eta_{prop}\, \eta_{motor}\, VI \tag{2.9}$$

$$C_t \rho n^2 D^4 v = \frac{C_t J}{C_p} C_p \rho n^3 D^5$$

$$v = JnD$$

$$v = \frac{v}{nD} nD$$

$$1 = 1 \tag{2.14}$$

The manipulation of the power equations holds true because simplification produces the true statement in Equation 2.14. Because of this, these equations may be freely substituted into each other in order to aid in performance analysis.

Returning to the example of the Turborix D2836 motor, these performance equations are used to find the unknown values of thrust, propeller efficiency, and axial propeller velocity using
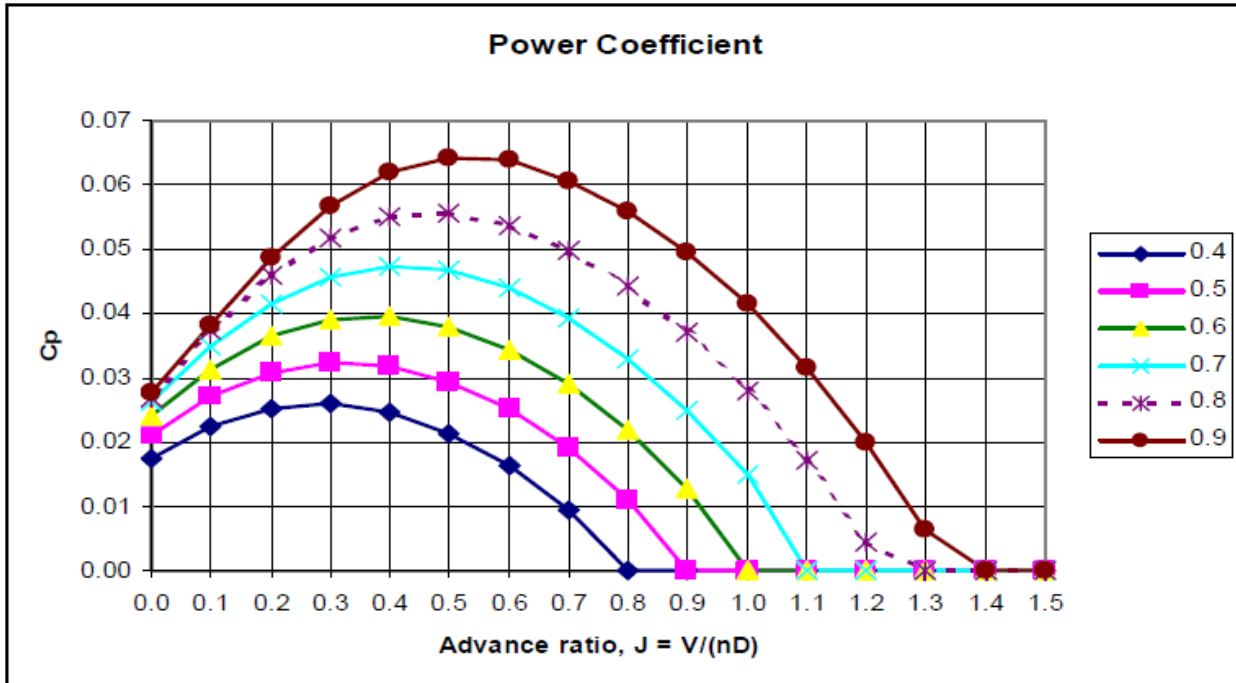
Figure 1.2: Plot of Power Coefficient vs. Advance Ratio for Varying Pitch to Diameter Ratios.
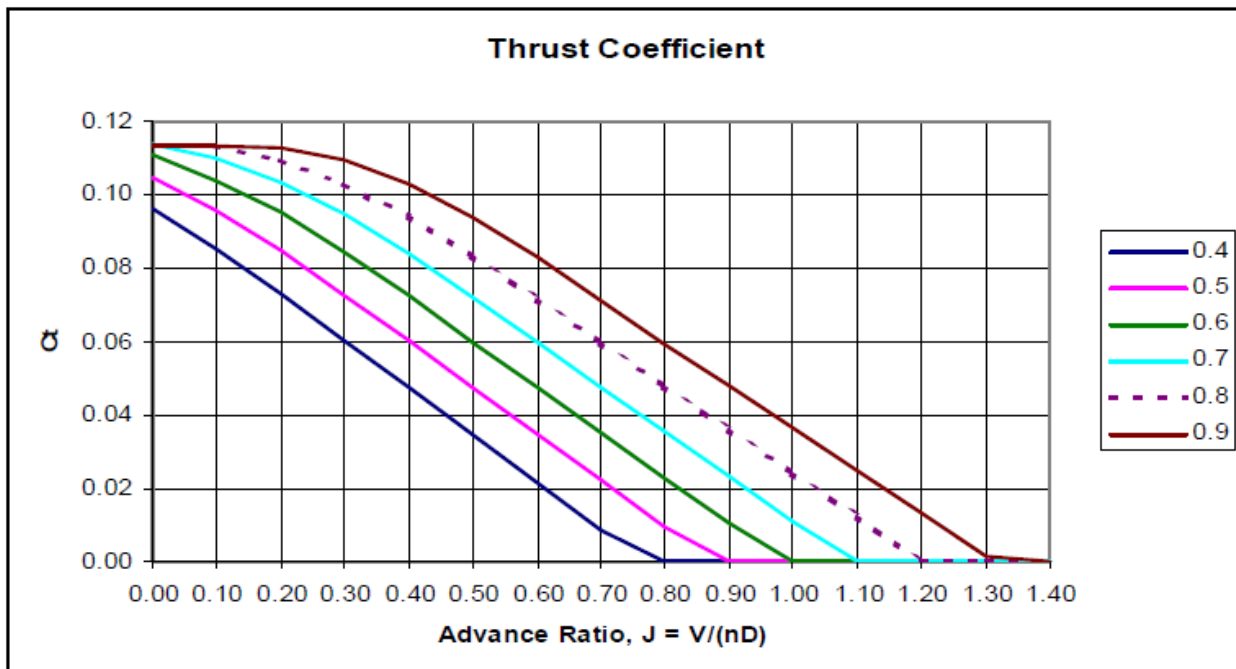Source: http://www.dc-rc.org/pdf/Model%20Propellers%20Article.pdf

Figure 2.3: Plot of Power Coefficient vs. Advance Ratio for Varying Pitch to Diameter Ratios.
Source: http://www.dc-rc.org/pdf/Model%20Propellers%20Article.pdf

the limited manufacturer specifications. First, determine the motor efficiency using Figure 2.1. For a motor with an input power of 355 W, the efficiency is 81.8%. This means that the output power, after being subjected to the efficiency factor is 290.62 W.

Next, find the power coefficient using the known output shaft power of 290.62 W (0.389 Horsepower) and revolution rate of 12,600 rpm. The D2836 manufacturer recommends using a 10×5 Electric propeller, meaning that the propeller has a 10 inch diameter and a 5 inch pitch—this propeller will be used for the calculations (this propeller has a pitch to diameter ratio of 0.5). Additionally, the air density will be assumed to be the standard sea level value of 0.002378 slugs per cubic feet. The coefficient of power can be calculated using equation 2.11:

$$0.390 \; hp = C_p \left(0.002378 \; {slug}/{ft^3} \right) \left(12600 \; rpm \cdot \frac{min}{60 \; sec} \right) \left(\frac{10 \; in}{12 \; {in}/{ft}} \right)^5 \left(\frac{1}{550 \; hp} \right)$$

$$C_p = 0.0242 \tag{2.15}$$

Because specifications are given in a mix of English and SI units, consistent units must be established in order to ensure that the final value for C_p is dimensionless. Referring to Figure 2.2, the advance ratio can be determined from this power coefficient and from the propeller's pitch to diameter ratio. From the plot, the advance ratio value is approximately 0.61. Using the definition of the advance ratio, the propeller's velocity can be determined by

$$0.61 = \frac{v}{\left(12600 \; rpm \cdot \frac{min}{60 sec} \right) \left(\frac{10 \; in}{12 \; {in}/{ft}} \right)}$$

$$v = 106.8 \; {ft}/{sec} \tag{2.16}$$

The axial velocity of the propeller is 106.8 ft/sec, or 72.82 mi/hr. This is not, however, the velocity of the entire aircraft because it does not include the drag effects of the airframe—it is simply the velocity of the air immediately behind the propeller. Next, using Figure 2.3, the thrust coefficient versus advance ratio for varying propeller dimensions, as a reference, c_t is approximated as 0.0340 using the advance ratio and pitch to diameter ratio of this specific

propeller. At this point, the total thrust produced by the propeller can be found using Equation 2.12 as

$$T = (0.034)\left(0.002378\,{}^{slug}\!\big/_{ft^3}\right)\left(12600rpm\,\frac{min}{60\ sec}\right)^2\left(10in\,\frac{ft}{12\ in}\right)^4$$

$$T = 1.72\ lbf \tag{2.17}$$

The total thrust produced by the propeller is measured as 1.72 lbf. The propeller's efficiency can also be calculated using the defined motor and propeller specifications with Equation 2.13:

$$\eta = \frac{(0.034)(0.61)}{(0.0242)} \times 100\% = 85.7\% \tag{2.18}$$

All components of this efficiency equation are dimensionless, which allows for a dimensionless resulting efficiency. The efficiency depends not only on the specifications of the propeller, but also on the motor shaft's rate of revolution, meaning that efficiency is not an intrinsic property of a given propeller. Alternately, the efficiency can be calculated using the primary relationship between the motor's power and the airplane's mechanical power by applying Equation 2.9:

$$(1.72\ lbf)\left(106.8\,{}^{ft}\!\big/_{sec}\right) = \eta(0.818)(0.4761hp)\left(\frac{550\left({}^{ft\,\cdot\,lb}\!\big/_{sec}\right)}{hp}\right)$$

$$\eta = 85.7\% \tag{2.19}$$

which is the same result as calculated in Equation 2.18.

Because each motor manufacturer provides a list of different specifications with their motors, there is no consistent method or order for determining the motor and propeller relationships. For example, some manufacturers specify voltage and rpm/V, from which the maximum rpm can be determined, while others supply rpm/V and the maximum rpm, from which the maximum voltage can be calculated. As a result, the analysis of each motor and propeller combination must be conducted individually. Overall, however, trends emerge in the data, such as the fact that most propellers have efficiencies in the range of 75% to 85%.

Because the motor and propeller are integral components which determine an aircraft's overall motion, the analysis has begun with these aircraft components. Once the characteristics

of the motor and propeller combination have been sufficiently evaluated and quantified, the scope of the analysis can be expanded to include the entire airframe. In the next section, the aerodynamics of the entire aircraft will be investigated. Afterwards, these aerodynamic results will be compared with the results from this section in order to assess aircraft performance.

Section 3

Airframe Drag Analysis

Drag is the aerodynamic force which acts opposite to an aircraft's thrust force and which opposes the aircraft's relative motion through the air. Drag pervades the study of aerodynamics because it arises from many different aspects of flight including friction between air and the aircraft skin material, a pressure differential between the front and rear parts of a body, energy loss due to the creation of air vortices, and large angles of attack which tilt part of the lift force in the rearward direction. The contribution of each type of drag must be assessed individually, and the total drag is the sum of each type of drag.

In general, drag can be divided into two categories: parasitic drag and induced drag. Parasitic drag (also called profile drag) is the rearward force experienced by a body as it moves through a fluid, in this case air and is comprised of numerous force effects. First, skin friction drag is the shear stress force caused by the interaction between the surface of the aircraft with the surrounding air, which results in energy loss in the form of heat. Second, pressure drag (or form drag) is the result of the pressure effects of air as it flows over a body. As air flows over an object, it separates, causing vertices of swirling air left in the object's wake. Compared to the high dynamic pressure of the oncoming air, the swirling vortices have low dynamic pressure (dynamic pressure is the pressure created by the force of the oncoming airflow acting on the frontal area of the body). In order to maintain equilibrium, this creates a net rearward force. The relative contributions of skin friction and pressure drag to the total parasite drag depend on the shape of the object. Skin friction drag is greatest for components which have a large surface area, such as wings. Pressure drag, however, is greatest for components with large frontal areas relative to their length (length is measured in the direction of the free stream). These shapes are called blunt bodies, and, due to their shape, can cause significant drag. For example, the total parasite drag of a radio controlled aircraft's wire landing gear strut (a blunt body) is approximately equal to the total parasite drag of the entire wing (a streamlined body generating predominately skin friction drag and very little pressure drag). Figure 3.1 displays the pressure
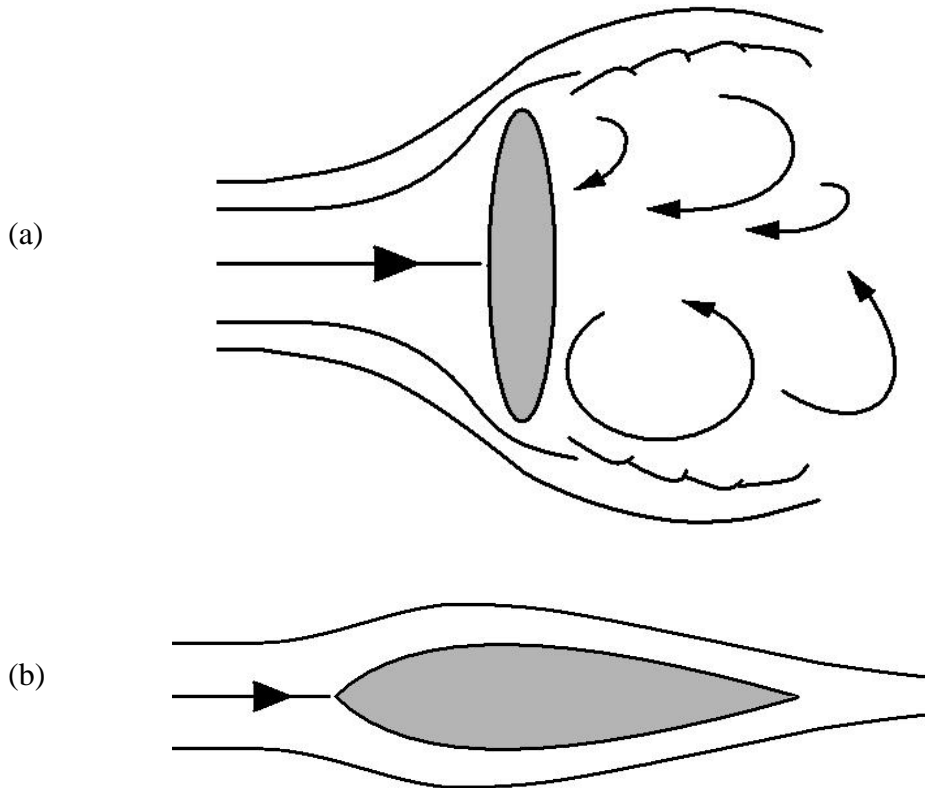
Figure 3.1: *(a)* Pressure Drag Due to Separation at a Blunt Body. *(b)* Skin Friction Drag Due to the Friction Interaction between Air and the Streamlined Airfoil Surface.

drag which occurs at a blunt body and the skin friction drag which occurs on a streamlined body.

While the skin friction and pressure drag can be approximated for each component of an aircraft, a third type of drag, interference drag, emerges when the proximity of these aircraft components is considered. Interference drag is caused by the relative airflows over different components of an aircraft: the flow over one part of an aircraft may disrupt the flow over another part. Parasitic drag, which is one of two components of total drag, is comprised of skin friction, pressure, and interference drag.

The second category of drag is induced drag, which is caused by the rearward component of the lift vector as the free stream is canted downward by a finite wing. The lift vector of an airfoil (considered an infinite wing) is orthogonal to the chord line of the airfoil, and at a zero angle of attack is also orthogonal to the free stream. For a finite wing, however, the pressure difference on the top and bottom of the wing surfaces encourages air to flow from the high pressure region to the low pressure region, creating wing vortices of circulating air. The vortices which occur at the wingtips produce a downwash of air behind the wing, which reduces the wing's effective angle of attack. In order to compensate, a higher angle of attack is required. As

15

the angle of attack increases, the lift vector remains orthogonal to the chord, but is no longer orthogonal to the free stream. With this greater angle of attack, a small component of the lift vector is directed in the rearward direction, which acts as a rearward force, thereby creating drag. The induced drag increases as an airfoil's angle of attack increases. The following equations list the relations between the different forms of drag:

Total Drag = Parasite Drag + Induced Drag

Parasite Drag = Skin Friction Drag + Pressure Drag + Interference Drag

When considering the sources of drag, a convenient method for analyzing the total drag emerges: the parasite drag can be approximated for each aircraft component, and then summed to determine the total parasite drag, which can then be added to the induced drag for the total aircraft. This is called the drag build-up method, and will be used for analyzing the radio controlled aircraft. Additionally, instead of finding the total drag for each component, a non-dimensional coefficient of drag will be determined which relates the drag of a given component to a common reference area (the planform wing area will be used as the reference area in all calculations). Similarly, the induced drag will be made non-dimensional using a coefficient of lift in which the same wing area will be used as a reference area. By substituting coefficients for the drag and lift terms, the total drag equation becomes

$$C_D \quad = \quad C_{D_P} \quad + \quad C_{D_I} \qquad\qquad (3.1)$$

<div align="center">

Total drag coefficient   Parasite drag coefficient   Induced drag coefficient

</div>

in which the total coefficient is simply the summation of the two components.

Using the drag build up method, the parasite drag coefficient term in Equation 3.1 becomes

$$C_{D_P} = \frac{Q}{S_{ref}} \sum_{i=1}^{n} \frac{K_i C_{f_i} S_{wet_i} q_{\infty_i}}{q_\infty}. \tag{3.2}$$

$$Q = \text{Drag interference factor}$$
$$S_{ref} = \text{Reference area}$$
$$K_i = \text{Form factor}$$
$$C_{f_i} = \text{Skin friction coefficient}$$
$$S_{wet_i} = \text{Total wetted area of the component}$$
$$q_{\infty_i} = \text{Dynamic pressure of the component}$$
$$q_\infty = \text{Free stream dynamic pressure}$$

This summation represents the method for finding the total parasite drag coefficient, which is the summation of the *n* total aircraft components.

This form of the parasite drag coefficient build-up equation contains numerous differences from that used for standard high Reynolds number aircraft. Most important is the inclusion of the dynamic pressure terms in the numerator and denominator terms of the summation. In converting from drag to drag coefficient, the drag term is divided by the dynamic pressure term as part of the effort to create a non-dimensional value for the drag coefficient. In most calculations, the dynamic pressure experienced by each aircraft component can be assumed to be equal to the dynamic pressure for the total aircraft, in which case the q_∞ terms cancel. In low Reynolds number aircraft, however, which tend to have high drag relative to their size and which usually have large propellers and power plants relative to their size, the dynamic pressure distribution is a significant element of the drag analysis. The dynamic pressure is defined as

$$q_\infty = \frac{1}{2} \rho_\infty V_\infty^2 \tag{3.3}$$

where ρ_∞ is the free stream air density and V_∞ is the free stream velocity. Given this definition, the dynamic pressure is proportional to the square of the free stream velocity (if the air density is held constant); the air velocity clearly has a significant effect on dynamic pressure. In low Reynolds aircraft, the relatively large propeller accelerates air passing through it, creating a wake

17

of accelerated air behind it. This accelerated air increases the dynamic pressure of aircraft components including the fuselage, horizontal and vertical stabilizers, and the landing gear struts. In large aircraft the effect of the propeller wake may be negligible, but in small aircraft the effect is significant. Additionally, the simplicity of construction of many radio controlled aircraft and RPVs means that they are not streamlined as well as full size aircraft, leading to greater drag effects as air from the propeller wake passes over the fuselage. To account for the effects of the greater dynamic pressure in the propeller's wake, an additional term is added to the dynamic pressure equation which accounts for the disc loading of the propeller:

$$q_{\infty_i} = \frac{1}{2}\rho_\infty V_\infty^2 + \frac{T}{A} \tag{3.4}$$

where T is the thrust force and A is the circular area of the propeller sweep. This increased dynamic pressure only applies to aircraft components which are within the propeller wake. For parts outside the wake, q_∞ is equal to q_{∞_i}, so the two terms cancel out, as normally occurs during drag coefficient calculations for higher Reynolds number aircraft.

The second discrepancy between the ordinary drag coefficient equation and Equation 3.2 is the method of incorporating the interference drag coefficient Q. Normally Q is part of the summation and is determined for each aircraft component. For small radio controlled aircraft, however, a single Q value is applied to the entire drag coefficient summation. This Q value accounts for both the interference between aircraft components and the additional drag created by small aircraft features which are not included in the drag build-up summation, such as servo horns and screw heads. For radio-controlled aircraft, values of Q range from 1.1 to 1.3.

In order to calculate the coefficient of parasite drag using the drag build-up method presented in Equation 3.2, the form factor K_i, skin friction coefficient C_{f_i}, and wetted area S_{wet} must first be determined for each aircraft component. The purpose of the form factor is to account for the thickness of the wing and fuselage on their equivalent parasite areas (it accounts for the ratio of thickness to length). The fuselage form factor is expressed as

$$K_f = 1 + \frac{60}{\lambda_f^3} + \frac{\lambda_f}{400} \tag{3.5}$$

where λ_f is the fineness ratio, which is defined as

$$\lambda_f = \frac{l_f}{D_f} \tag{3.6}$$

where l_f is the fuselage length and D_f is the fuselage diameter. A different expression represents the form factor for a wing:

$$K_w = 1 + Z\left(\frac{t}{c}\right) + 100\left(\frac{t}{c}\right)^4 \tag{3.7}$$

in which t is the airfoil thickness and c is the airfoil chord length. Additionally, Z is the sweep correction factor, which depends on wing sweep angle and Mach number. For radio controlled aircraft with no wing sweep and very low Mach numbers, the value of Z can be approximated as 2. The wing form factor equation can also be applied to the horizontal and vertical stabilizers. For other aircraft components, including the landing gear strut and tires, the value of K can be assumed to be 1.

Next, the skin friction coefficient is used as a means of quantifying the friction due to the viscous effects of a flow over an exposed surface. The Schlichting formula for the skin friction coefficient estimates the value as

$$C_f = \frac{0.455}{(\log Re)^{2.58}} \tag{3.8}$$

for surfaces in a boundary layer which is predominantly turbulent. This formula is satisfactory for estimating the skin friction coefficient on all aircraft components.

The last element of completing the drag build-up analysis is the calculation of S_{wet}, the total wetted area. The wetted area is the total surface area of a given aircraft component which is exposed to the airflow. Because measuring the wetted area is difficult, a number of equations can be used to estimate the wetted areas of various aircraft components. If the fuselage is modeled as a cylinder with rounded ends, the total exposed area can be calculated with

$$S_{wet_f} = \pi D_f l_f \left(1 - \frac{2}{\lambda_f}\right)^{2/3}\left(1 + \frac{1}{\lambda_f{}^2}\right) \tag{3.9}$$

and the wing's wetted area can be estimated as

$$S_{wet\,w} = S_w \cdot 2 \cdot 1.02 \tag{3.10}$$

where S_w is the wing planform area. In Equation 3.10, the planform wing area is multiplied by 2 to account for both sides of the wing, and is then multiplied for 1.02 to account for the wing's thickness. Equation 3.10 can also be used for finding the wetted area of vertical and horizontal stabilizers. For other aircraft components, including tires and the landing gear strut, the total wetted areas are simply calculated as the surface areas of representative geometric shapes.

Equation 3.2 estimates the total parasitic drag coefficient for low Reynolds number aircraft. At this point the parasite drag coefficient can be entirely calculated and the next step toward determining the overall drag coefficient is to calculate the induced drag coefficient. The coefficient of induced drag is

$$C_{D_I} = \frac{C_L{}^2}{\pi e \text{AR}} \tag{3.11}$$

where e is the span efficiency factor, and AR is the wing's aspect ratio. These two terms must be added to the induced lift term to compensate for the lift distribution of a finite wing with a given planform shape. The aspect ratio of the wing is a measure of the relative width and chord length and is defined as

$$\text{AR} = \frac{b^2}{s} \tag{3.12}$$

where b is the wingspan and s is the planform wing area.

Induced drag is an effect of lift and angle of attack, and therefore must be calculated for every lift-producing surface. This analysis will consider the induced drag effect of the wing and fuselage. While the wing provides the majority of the aircraft's lift, the minor lifting effect of the fuselage must also be factored into the calculation. Accounting for the horizontal stabilizer is unnecessary: the horizontal stabilizer is located in the wing's downwash, which limits its lifting capability. The total span efficiency factor for the airplane is

$$\frac{1}{e_{total}} = \frac{1}{e_w} + \frac{1}{e_{fus}} + 0.05 \tag{3.13}$$

in which e_w is the fuselage form factor, e_{fus} is the wing form factor, and 0.05 accounts for the form factor of other aircraft components. The value for e_w is dependent upon the wing's shape; for the rectangular wing designs frequently used for radio controlled aircraft, the value is usually between 0.7 and 0.8. Figure 3.2 is a plot of the wing form factor value as a function of the wing aspect ratio. The value of e_{fus} is calculated from the shape and cross sectional area of a fuselage. Figure 3.3 displays the fuselage efficiency factor for round fuselages with cowled power plants, as are commonly used in radio controlled aircraft designs. In order to plot the fuselage efficiency factor as a function of the wing aspect ratio, the e_{fus} values must be related to the wing area S. Additionally, the e_{fus} term is divided by the fuselage cross sectional area S_{fus} to account for the size of the fuselage. Because of these two complications, the quantity on the vertical axis in Figure 3.3 is

$$\frac{\Delta\left(\frac{1}{e_{fus}}\right)}{S_{fus}/S} \tag{3.14}$$

from which the value of e_{fus} alone can be obtained.

The final calculation needed for the coefficient of induced drag analysis is the coefficient of lift. Similar to the relationship between drag coefficients and total drag, the coefficient of lift is a method of determining a non-dimensional value which relates the total lift to a reference area. For straight and level flight, the coefficient of lift is expressed as

$$C_L = \frac{W}{q_\infty S_{ref}} \tag{3.15}$$

where W is the aircraft's weight. The weight is used because, for straight and level flight, the total lift force is equal in magnitude to the weight force. The denominator of coefficient of lift equation serves to make the value non-dimensional and relate it to the reference area.

A trial drag build-up analysis will now be conducted for the AirLandSea Hobbies ARF Kitman electric-powered radio-controlled airplane. This aircraft utilizes the Turborix D2836 Brushless motor and 10×5 propeller which were analyzed in the previous section. For this analysis, assume a velocity of 15 m/s (33.6 mi/hr). The first step is to calculate the parasite drag for each aircraft component, including the fuselage, wing, horizontal and vertical stabilizers,
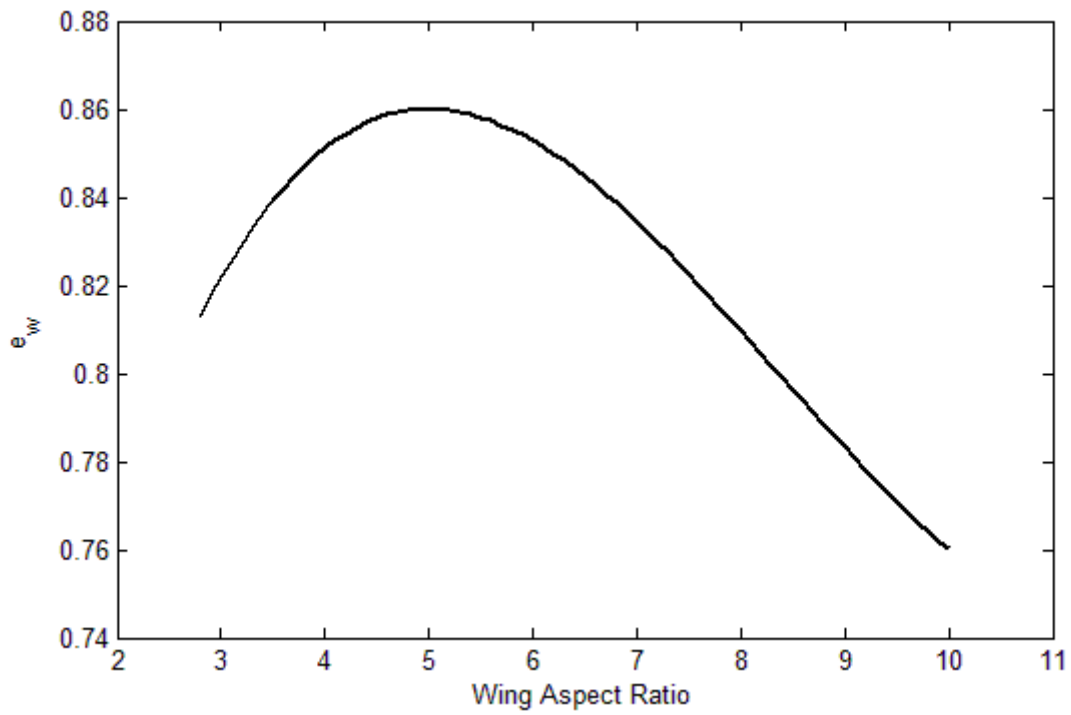
Figure 3.2: Efficiency Factor of a Rectangular Wing with Increasing Aspect Ratio.
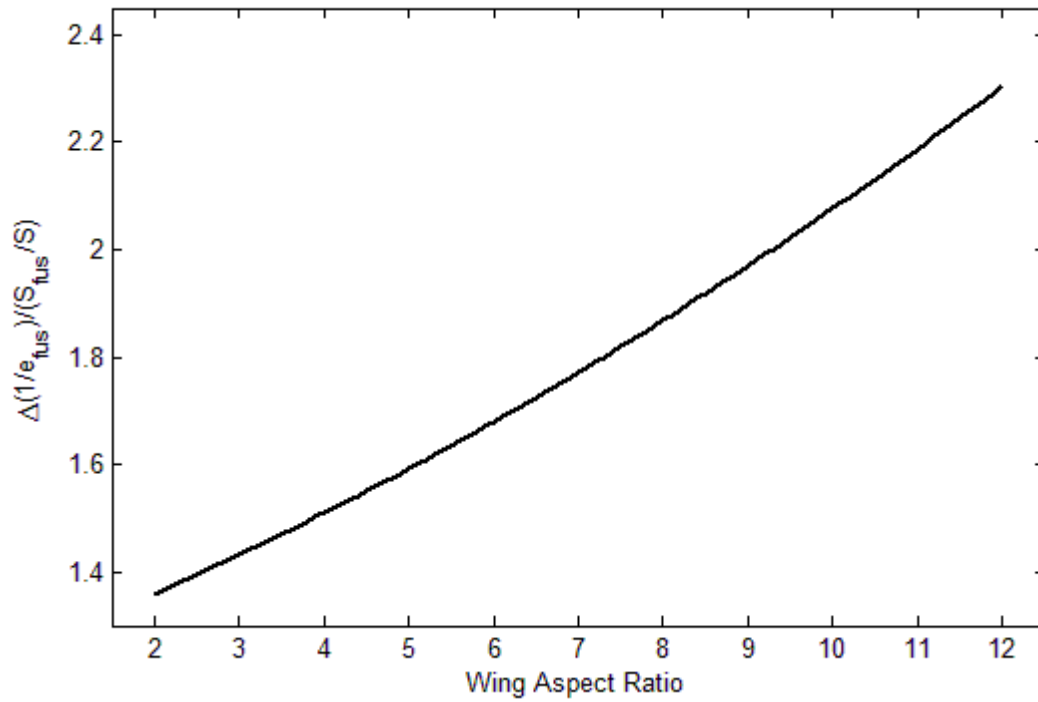

Figure 3.3: Efficiency Factor of a Round, Cowled Fuselage with Increasing Aspect Ratio.

landing gear strut, and tires. While the relative size of the strut and tires is small, their contribution to the parasite drag coefficient is significant due to their blunt body shape. Calculations are shown for the fuselage: referencing Equation 3.2, the first element of the summation which must be calculated is the form factor. The fuselage form factor depends on the fuselage fineness ratio in Equation 3.6. Using the manufacturer-specified length of 0.96 m and the approximated diameter of 0.14 m, t fineness ratio is

$$\lambda_f = \frac{0.96\ m}{0.14\ m}$$

$$\lambda_f = 6.86 \tag{3.16}$$

This value is next used in Equation 3.5 to determine the form factor:

$$K_f = 1 + \frac{60}{6.86^3} + \frac{6.86}{400}$$

$$K_f = 1.20 \tag{3.17}$$

The next element of Equation 3.2 which must be calculated is the skin friction coefficient. This quantity relies on the Reynolds number, which must first be determined using the definition of the Reynolds number. Assuming an air density of 1.225 kg/m^3 and viscosity of 1.789×10^{-5} kg/m·s, the Reynolds number is

$$Re = \frac{\left(1.225\ ^{kg}/_{m^3}\right)(15\ ^m/_s)(0.960\ m)}{\left(1.789 \times 10^{-5}\ ^{kg}/_{m \cdot s}\right)}$$

$$Re = 9.860 \times 10^5 \tag{3.18}$$

Now the skin friction coefficient can be calculated from Equation 3.8:

$$C_f = \frac{0.455}{[\log(9.860 \times 10^5)]^{2.58}}$$

$$C_f = 0.00448 \tag{3.19}$$

Both the Reynolds number and the skin friction coefficient are dimensionless, as can be confirmed by canceling the units in each calculation. The fuselage wetted area must be calculated next. Equation 3.9 provides a simple approximation for the wetted area assuming a cylindrical fuselage with rounded ends. Substituting the fuselage diameter, length, and fineness ratio, the wetted area is

$$S_{wet_f} = \pi(0.14m)(0.96m)\left(1 - \frac{2}{6.86}\right)^{2/3}\left(1 + \frac{1}{6.86^2}\right)$$

$$S_{wet_f} = 0.343m^2 \tag{3.20}$$

The total surface area of the fuselage which is exposed to the airflow is approximately 0.343m^2. The final two elements of the summation in Equation 3.2 which must be determined are q_∞ and q_{∞_i}, the two dynamic pressure terms. Because the fuselage is located in the propeller's slipstream, it will experience a greater dynamic pressure meaning that q_∞ and q_{∞_i} are not equal. For aircraft components located outside the propeller wake, such as the wing, the two dynamic pressure terms simply cancel. The free stream dynamic pressure outside the slipstream is calculated with Equation 3.3:

$$q_\infty = \frac{1}{2}\left(1.225 \; {}^{kg}\!/_{m^3}\right)(15 \, {}^m\!/_s)^2$$

$$q_\infty = 137.8 \, Pa \tag{3.21}$$

Without factoring any the effect of the slipstream, the dynamic pressure is 245 Pa. Next, the dynamic pressure must be calculated using Equation 3.4. Using the thrust value of 1.72 lbf (7.65 N) and the propeller diameter of 10 in (0.254 m), the slipstream dynamic pressure is calculated as

$$q_{\infty_i} = \frac{1}{2}\left(1.225 \; {}^{kg}\!/_{m^3}\right)(20 \, {}^m\!/_s)^2 + \frac{7.65 \, N}{\frac{\pi}{4}(0.254 \, m)^2}$$

$$q_{\infty_i} = 288.8 \, Pa \tag{3.22}$$

The dynamic pressure in the slipstream is approximately 62% greater than the free stream dynamic pressure. Because of the relatively large motor and propeller relative to the fuselage size, accounting for the slipstream dynamic pressure difference can lead to more accurate drag predictions.

Using the summation term in Equation 3.2, the total coefficient of parasite drag for the fuselage can be calculated. This calculation utilizes the results of all the of sub-calculations which were previously determined; substituting these values yields

$$C_{D_{P_f}} = \frac{(1.20)(0.00425)(0.343 m^2)(288.8\ Pa)}{(137.8\ Pa)}$$

$$C_{D_{P_f}} = 0.00367\ m^2 \tag{3.23}$$

The resulting fuselage drag value is 0.00367 m^2; however, this value is not dimensionless. In the final step of the parasite drag coefficient build-up, the summed drag from each aircraft component (each with units of square meters) will be referenced back to the wing area and will be made dimensionless.

By repeating the parasite drag build-up process for the wing, tail assembly, landing gear strut, and tires in a similar method to that presented for the fuselage, the total drag value (relative to the summed wetted area of the components) for each component can be calculated. After summing the parasite drag contribution from the fuselage, wing, tail assembly, and two tires, the total drag value is 0.0434 m^2. The final two steps consist of applying a drag interference factor (which also accounts for miscellaneous drag) and then dividing by the reference area (the wing area is 0.209 m^2), which makes the drag value non-dimensional by relating the areas of each aircraft component to the wing area. A reasonable value for the interference factor Q is 20%, meaning that the total drag coefficient must be multiplied by 1.2 to account for the additional drag. Implementing Q and the reference area, the total coefficient of parasite drag is

$$C_{D_P} = \frac{1.2}{0.209\ m^2}(0.0434\ m^2)$$

$$C_{D_P} = 0.2492 \tag{3.24}$$

The final coefficient of parasite drag for the entire airplane at 15 m/s is estimated to be 0.2492. This value is non-dimensional, which increases its versatility and means that any further analysis can be conducted using any consistent set of units.

The next step toward determining the total coefficient of drag is to find the coefficient of induced drag. The first quantity which needs to be calculated is the aspect ratio, given in Equation 3.12; substituting the values for the Kitman ARF, the aspect ratio is

$$AR = \frac{(1.10m)^2}{0.209 \; m^2}$$

$$AR = 5.79 \tag{3.25}$$

Now the total span efficiency factor can be calculated from the fuselage and wing efficiency factors. From Figure 3.2, the span efficiency for a rectangular wing with an aspect ratio of 5.79 is 0.86. Additionally, from Figure 3.3, the fuselage efficiency value relative to the wing area is 1.66 given a 5.79 aspect ratio. Using the relationship established in Equation 3.14, the span efficiency of the fuselage can be obtained (assuming a circular fuselage cross-section):

$$\frac{\Delta\left(\frac{1}{e_{fus}}\right)}{\left(\frac{\pi}{4}\right)(0.14m)^2 \Big/ 0.209 \; m^2} = 1.66$$

$$\Delta\left(\frac{1}{e_{fus}}\right) = 0.122 \tag{3.26}$$

Because the method of combining the wing and fuselage span efficiencies involves summing their inverses, finding the inverse of the fuselage efficiency factor is sufficient for now and will simplify calculations later when finding the total efficiency factor for the aircraft. The delta sign indicates that the reciprocal of the fuselage efficiency factor is the amount by which the reciprocal of the wing efficiency factor is changed. Using Equation 3.13 as a reference, the total efficiency factor is

$$\frac{1}{e_{total}} = \frac{1}{0.86} + 0.122 + 0.05$$

$$e_{total} = 0.749 \tag{3.27}$$

The approximate efficiency factor for the entire airframe is 0.749.

The last quantity which must be calculated before finding the induced drag coefficient is the coefficient of lift, which is defined in Equation 3.15. The weight of the Kitman ARF is 4.86 N. By substituting values, the coefficient of lift is

$$C_L = \frac{4.86\ N}{(137.8\ Pa)(0.209\ m^2)}$$

$$C_L = 0.169 \tag{3.28}$$

which is necessarily non-dimensional. Now the aspect ratio, efficiency factor, and coefficient of lift can be used to determine the coefficient of induced drag, using Equation 3.11 as a reference:

$$C_{D_I} = \frac{(0.169)^2}{\pi(0.749)(5.79)}$$

$$C_{D_I} = 0.00210 \tag{3.29}$$

The total coefficient of drag is simply the sum of the parasite coefficient and the induced coefficient:

$$C_D = 0.2492 + 0.00210$$

$$C_D = 0.2513 \tag{3.30}$$

The total coefficient of drag at 15 m/s is 0.2513; again, this value is non-dimensional but is representative of the total drag.

At this point, the total coefficient of drag, consisting of the coefficient of parasite drag and the coefficient of induced drag, can be calculated for a given radio controlled aircraft. The total coefficient of drag can now be converted into the total drag force by relating the coefficient to the reference area. By doing this, the total drag can easily be extracted from the coefficient of drag. In converting between drag and drag coefficient, the functionality of the coefficient of drag is evident: by establishing a non-dimensional value which is related to a standard reference area, the drag between aircraft components and between separate aircraft can easily be compared.

Section 4

Performance Analysis

Fully understanding the performance characteristics of a proposed aircraft design is integral to ensuring the feasibility of the aircraft. The various performance parameters, including maximum velocity, range, and ceiling, dictate flight behavior and are rooted in the basic aerodynamic forces of lift and drag and in their relationship to weight and thrust. The performance of an aircraft is based on its aerodynamics. In this manner, the drag data from Section 3 can be used to predict the fundamental performance capabilities for aircraft. The primary link between aerodynamic characteristics and performance characteristics is the drag polar, a plot of the total coefficient of drag as a function of the coefficient of lift. In order to fully understand the method of establishing a drag polar and its applications, the significance of the drag coefficients in the previous section must first be further developed.

The primary concepts explained in Section 3 were the coefficient of parasite drag, the coefficient of induced drag, and their sum, the total coefficient of drag. These quantities are representative of the total drag, but do not, when used alone, quantify the total drag force experienced by an aircraft. However, the coefficients of drag can easily be related to the total drag force with

$$D = C_d q_\infty S_{ref} \qquad\qquad (4.1)$$

where D is the total drag force. The rationale of Equation 4.1 is fairly simple: in Section 3, a force quantity was divided by the reference area and by the dynamic pressure, which resulted in a non-dimensional quantity. Now, to convert back to the drag force, the coefficient of drag is multiplied by the reference area and the dynamic pressure. Because there are numerous velocity terms in the drag calculation process, the total drag force is dependent upon velocity (the calculations in Section 3 assumed a velocity of 15 m/s). The variation of drag with velocity is more apparent if the total drag force is broken into its two components: parasite drag and induced drag. Parasite drag is caused by the friction force and pressure differential as air passes over a

body, meaning that greater velocities result in a more pronounced parasite effect and greater drag. Induced drag, however, is a consequence of the finite wing's angle of attack. In order to maintain sufficient lift at low airspeeds, an aircraft's angle of attack increases, resulting in higher induced drag at low airspeeds. Mathematically, this is due to the q_∞ term in the denominator of the coefficient of lift C_L. When C_L is squared to calculate the induced drag coefficient, the velocity term in the denominator is taken to the fourth power. Despite the induced drag coefficient being multiplied by q_∞ to find the total induced drag force, the velocity term in the denominator still dominates, resulting in greater induced drag at low velocities.

The next step toward achieving a performance analysis is to consider the mechanical power associated with the drag force. The fundamental equation for mechanical power is

$$P = Fv \tag{4.2}$$

where F is the force associated with movement. The power which is required for an aircraft to maintain a constant velocity during level flight is equal to the drag force multiplied by the velocity. For level, unaccelerated flight, the thrust force equals the drag force, and therefore the power required by the propeller is equal to the power associated with the drag. When the terms are combined, the equation for power required is

$$P_{req} = \frac{1}{2}\rho S_{ref} v^3 \left(C_{D_P} + C_{D_I}\right) \tag{4.3}$$

Figure 3.4 displays the power required as a function of velocity for a typical radio-controlled aircraft. Additionally, the component of the total power required due to parasite drag and the component due to induced drag are illustrated (their sum is the total power required).

To investigate the performance of an aircraft, the power which is required must be compared to the power which is available—the power produced by the propeller. The output power is calculated in Section 2 and is considered constant with aircraft velocity. The power available line is plotted in Figure 3.4. When the power required and the power available graphs are plotted simultaneously, the resulting graph can give significant insight into the aircraft's performance. In order for the aircraft to have sufficient power to maintain a constant velocity, the power available must be greater than or equal to the power required. As a result, the velocity at which the power available is equal to the power required is the aircraft's maximum velocity
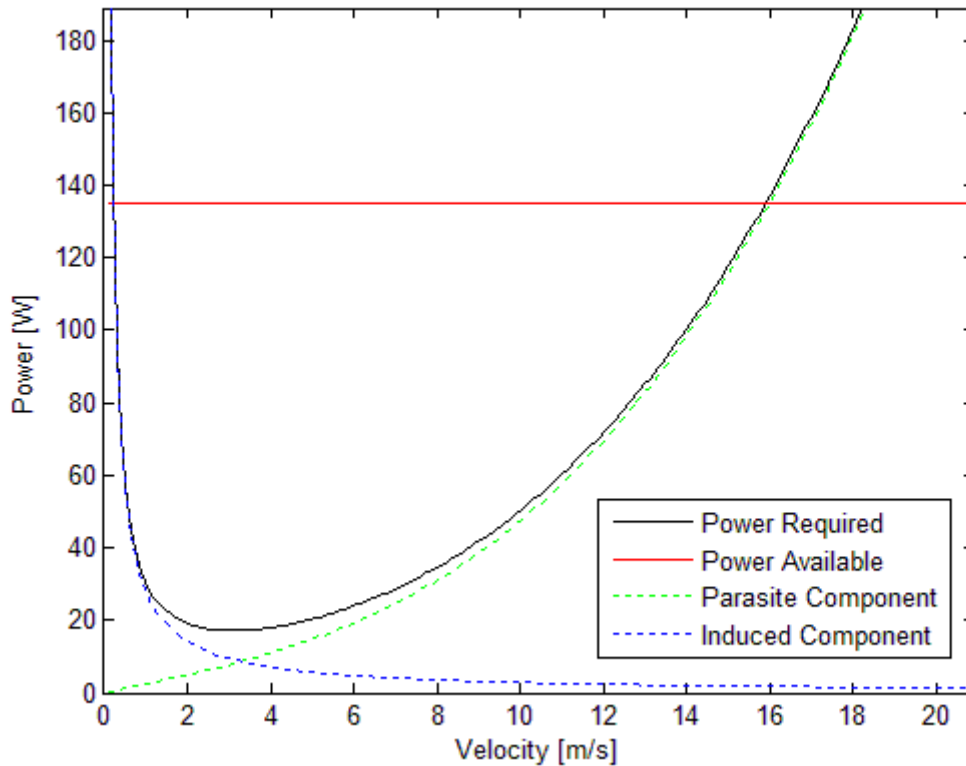
Figure 3.4: Sample Plot of Power Required and Power Available as Functions of Velocity, Including the Parasite and Induced Components of the Total Power Required.

during level flight. In order to maintain this maximum velocity, the aircraft must fly at full throttle, a fairly intuitive notion. An important observation from Figure 3.4 is that, in addition to a maximum velocity, there is a nonzero minimum velocity. Because the induced drag increases as velocity decreases, there exists a minimum flight velocity; below this velocity, the power required is greater than the power required. The graph suggests that, in order to maintain this minimum flight speed, full throttle is required. For the range of velocities where the power available is greater than the power required, the aircraft has excess power available. In this range, the aircraft can maintain a constant velocity without applying maximum power. In addition, the margin between the power required and the power available gives a measure of this excess power available if full throttle is applied. This excess power can be used to accelerate or climb. As is observed from Figure 3.4, the velocity at which the parasite drag component and induced drag component are equal also has significance. This is the velocity where the minimum power is required (the aircraft experiences the lowest drag force), and the corresponding
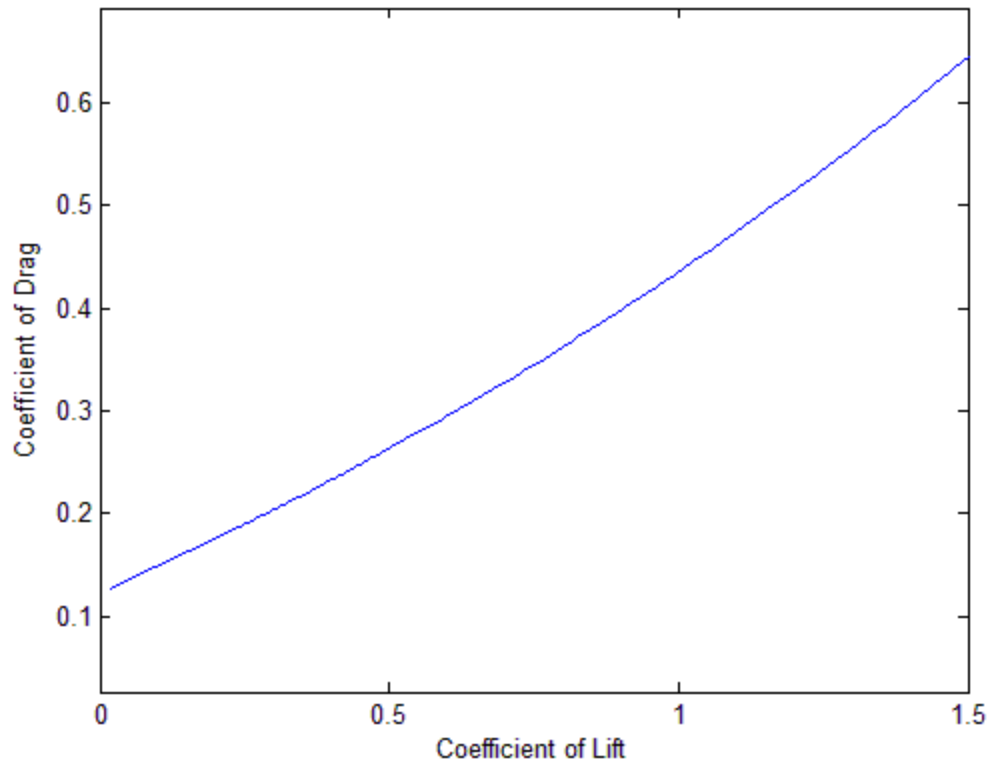
30

Figure 3.5: Sample Drag Polar, Indicating the Relationship Between Coefficient of
Lift and Coefficient of Drag.

minimum power can also be determined from the plot. A plot of the available and required powers as functions of velocity is an integral component of initiating a performance analysis of an aircraft.

At this point, the performance analysis will return to the subject of drag polar plots, another important means of assessing aircraft performance. A drag polar is a plot of the coefficient of lift as a function of coefficient of drag: a sample drag polar is represented in Figure 3.5. The coefficient of drag increases as the coefficient of lift increases. The coefficient of drag which corresponds to zero lift is C_{D_0} and is the lowest drag coefficient value for the aircraft. In order to generate an efficient and aerodynamic aircraft, the value of C_{D_0} should be as low as possible. Additionally, the coefficient of drag should increase as little as possible as the coefficient of lift increases. A drag coefficient which increases rapidly with increases in the lift coefficient indicates an inefficient aircraft design. As has been previously noted, radio

31

controlled aircraft rend to have relatively poor drag characteristics due to the simplicity of their design and construction. This results in large relatively coefficients of drag.

By comparing the power available and the power required as functions of velocity and by relating the coefficients of lift and drag, the fundamental performance parameters can be quantified and analyzed. These plots are an ideal method of studying the feasibility of a new aircraft design: the data presented in these two plots gives a preliminary idea of the proposed aircraft's performance. From the estimates achieved with these graphs, the aircraft's design can be altered in order to achieve the desired performance parameters. Additionally, in discussing performance, the tradeoffs which are inherent in aircraft design must be considered. For any given aircraft, certain performance specifications must be balanced with the design constraints, which may include payload, range, or fuselage size. In general, the performance analysis is the primary method of relating the aerodynamics of an aircraft to its basic flight behavior; in this sense, studying an aircraft's performance is an integral component of aircraft design and analysis.

Section 5

Results

The aerodynamic and performance equations developed in the preceding sections were applied to a database of radio controlled aircraft in order to determine the drag and performance characteristics for each aircraft. Additionally, the results from all aircraft were compared in an attempt to recognize trends in the data. Initially, a database of radio controlled aircraft, along with the dimensions and specifications for each aircraft, was established. According to Section 1, the aircraft which were incorporated into the database met a set of design criteria (including construction style, and power plant type) in order to ensure consistency in the results. However, a variety of aircraft sizes was selected in order to promote visible trends in the data results. In addition to the aircraft dimension database, a motor specification database was created, which included the maximum voltage, maximum current, and maximum rpm for each motor. The basic specifications for each aircraft were obtained from the aircraft manufacturer's website. As described in Section 1, the dimensions which were not specified by the manufacturer were estimated by analyzing reference photos of the aircraft and relating the unknown dimension to a known dimension. A sample reference photo is displayed in Figure 5.1; from photos similar to this one, unknown dimensions can be approximated in a relatively accurate manner. The completed database includes approximately thirty aircraft, and can easily be expended with additional aircraft.

After establishing the aircraft and motor databases, a program was written in Matlab which uses the equations and techniques presented in Sections 2, 3, and 4 in order to create a full drag and performance analysis for a given aircraft. A complete listing of the Matlab program code appears in Appendix A. The program functions by running the analysis for a single, user-defined aircraft from the database. After completing the analysis, the program creates a plot of power required and power available as functions of flight velocity and a separate plot of the drag polar. From these two plots, the performance parameters of the individual aircraft can be studied. Additionally, the program outputs several useful power plant and aerodynamic parameters. A sample output, which includes the output parameters, appears in Figure 5.2.

Figure 5.1: Reference Photo of the E-Flite Alpha 450 Sport ARF Aircraft, Illustrating the Method of Using Relative Sizes to Find Unknown Dimensions.
Source: http://www.rc-airplane-world.com/image-files/alpha-450-arf.jpg

```
>> rcairplane
Input the number which corresponds to the aircraft which you
would like to analyze: 9
Aircraft Analysis Results:
Total Thrust: 4.3667 N
Propeller Efficiency: 78.3743 %
Power Available: 251.8404 W
Minimum Power Required: 26.8883 W
Maximum Velocity: 24.6 m/s
```

Figure 5.2: Sample Matlab Output for an aircraft in the database.

While running the Matlab program for various aircraft from the database, several characteristics are elucidated which are specific to low Reynolds number aircraft. Because of compensating for the increased dynamic pressure in the propeller slipstream (which is particularly important in low Reynolds number aircraft, as explained in Section 3), the shape of both the power required and available plot and the drag polar plot are changed. By increasing the dynamic pressure over specific aircraft components which are in the slipstream (the fuselage, tail, landing gear struts, and tires), the parasite drag (and parasite drag coefficient) associated with those components is increased. Figure 5.3 displays the effect of the slipstream compensation by comparing the power required plots with and without the increased dynamic pressure. In the plot, the power required due to parasite drag is significantly increased (due to an increase in the coefficient of parasite drag) when slipstream compensation is introduced. Parasite drag is dependent upon velocity; when the velocity of the air is increased behind the propeller (reflected in the increased dynamic pressure), the parasite drag increases. Because of the increase in parasite drag and power required, the maximum airspeed decreases substantially. Additionally, the minimum power required is raised slightly. Because the margin between the
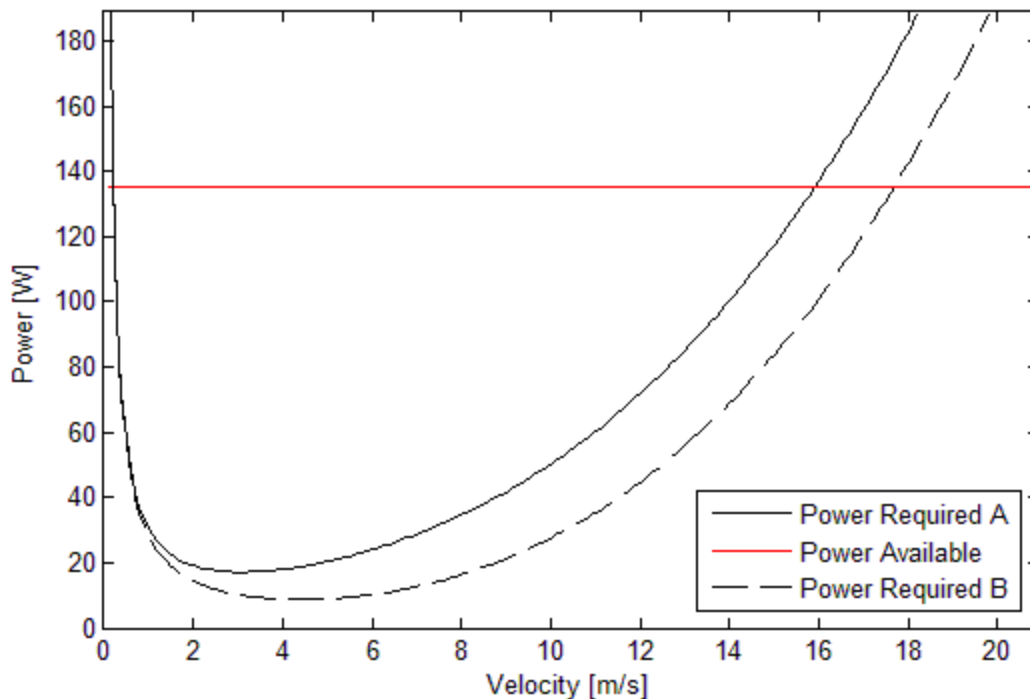

Figure 5.3: Power Required and Available Plot Showing the Effect of the Slipstream. Curve A Includes the Effect of the Slipstream, while Curve B ignores its effect.

power required and the power available is decreased at flight speeds where parasite drag dominates, the aircraft's ability to climb and accelerate is also hindered when the slipstream effect is considered. Figure 5.3 also demonstrates that, while increasing the dynamic pressure has an effect on parasite drag, it has essentially no effect on induced drag. Induced drag is caused by the angle of attack of the finite wing, which is predominately determined by the free stream velocity and the wing design. The majority of the wing is not affected by the propeller slipstream, and therefore is not dependent upon increasing the dynamic pressure. This trend is also reflected in the calculation of induced drag: in calculating the induced drag coefficient, the only calculation which depends on the dynamic pressure q_∞ term is that for the coefficient of lift. However, this coefficient of lift term measures the dynamic pressure experienced by the wing, which is simply the free stream dynamic pressure with no slipstream compensation. Additionally, this term cancels with the q_∞ term which is used to convert the induced drag coefficient into the total induced drag force. Because of this, the induced drag is mathematically independent of the velocity increase which occurs in the slipstream behind the propeller.

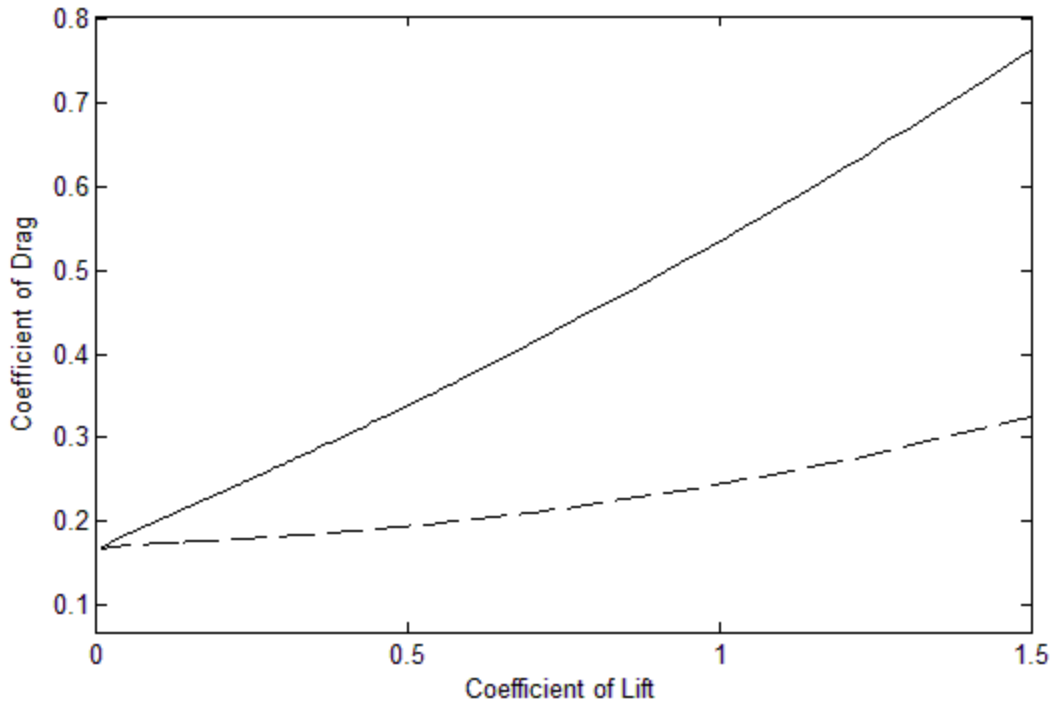Figure 5.4 demonstrates the effect of the slipstream dynamic pressure by plotting a

Figure 5.4: Drag Polar Plot Showing the Effect of the Slipstream. The Solid Curve Incorporates the Slipstream Effect, while the Dashed Curve Ignores its Effect.

sample drag polar with and without considering the slipstream. Both of the drag polar curves have a common drag coefficient at zero lift (C_{D_0}). This is a result of the fact that, due to limited airfoil data available for radio-controlled aircraft, the coefficient of lift was measured as a function of velocity. As a result, the C_{D_0} value corresponds to a velocity of zero.

First consider the lower curve in the drag polar plot, which does not incorporate the effect of the slipstream. If the axes in the plot in Figure 5.4 are changed such that the graph only displays the lower curve (the curve which does not account for the slipstream), the plot will follow the normal shape of a drag polar. This is reflected in Figure 5.5. The curve in Figure 5.5 is the same as the lower curve in Figure 5.4; however, the axes have been redefined to better preserve the curve's shape. The normal shape of a drag polar can be approximated by a positive exponential function (this applies only to the right-hand portion of the plot, which corresponds to positive values for the coefficient of lift), in which the slope of the curve increases as the coefficient of lift increases. For reference, Figure 5.6 displays a typical drag polar plot for a full-scale aircraft; this specific plot is for the NACA 0012 and NACA 66-415 airfoils. While the shape of the drag polar in Figure 5.5 follows the typical drag polar trend, the value of C_{D_0} is higher than that for most full scale aircraft. This is due to the relatively high parasite drag of
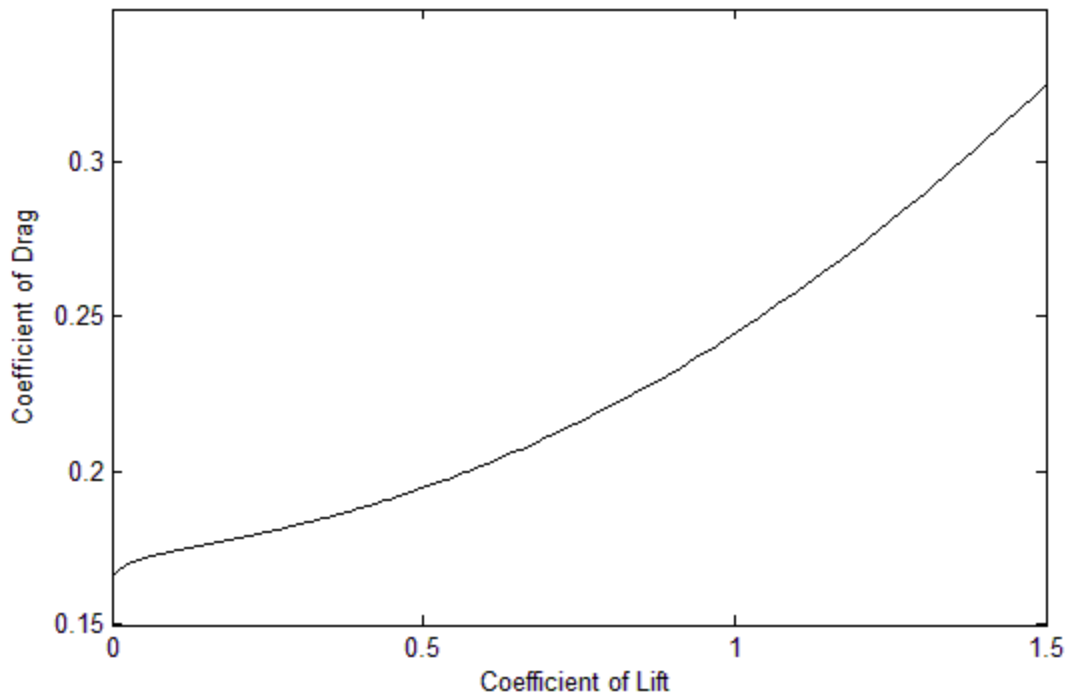

Figure 5.5: Drag Polar Plot without Considering the Effect of the Slipstream.
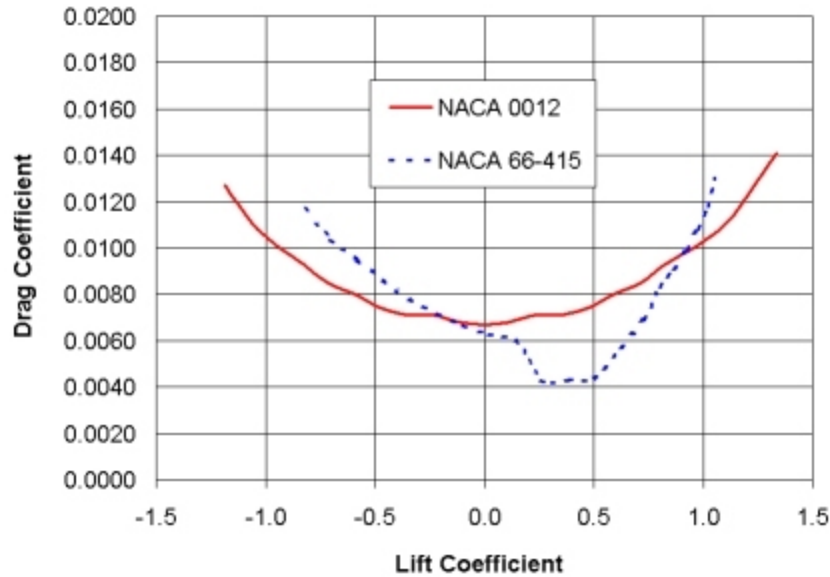
Figure 5.6: Typical Drag Polar for a Full-Scale Aircraft, Including the Range with Negative Values for Coefficient of Lift. Includes Information for NACA 0012 airfoil and NACA 66-415 Airfoil.

Source: http://www.dreesecode.com/primer/p3_f004.jpg

small, radio-controlled aircraft (even when the slipstream's effect on dynamic pressure is ignored). When the slipstream is ignored, the increase in the coefficient of drag as the coefficient of lift increases is due only to the induced drag, which is lift-dependent. In aircraft with significant induced drag, the rate at which the coefficient o drag increases will be greater than in aircraft with lower induced drag. Note that this analysis has concerned the lower curve. The next step toward fully understanding the drag polar is to consider the effect of the slipstream, which accounts for the difference between the two curves in Figure 5.4.

When the slipstream is incorporated into the analysis, new trends in the drag polar's shape emerge. The analysis will now consider the upper curve in Figure 5.4. As the coefficient of lift increase, the coefficient of drag of the upper curve increases more rapidly than does the lower curve. This is due to the greater parasite drag coefficient which occurs at greater velocities when the slipstream is considered. The increase in the drag coefficient due to the slipstream follows a linear trend as the coefficient of lift is increased. This is reflected in the shape of the upper curve in Figure 5.4, which is approximately linear. The drag coefficient increases linearly due to the nature of the equations which define the slipstream dynamic pressure. Additionally, because of the significant increase in parasite drag due to the slipstream effect, the shape of the

38

drag polar becomes dominated by the linear slipstream trend. This means that the induced effect is minor in comparison, resulting in a drag polar with a somewhat linear shape. In aircraft with significant induced drag, a somewhat limited curvature is still perceptible in the drag polar. In total, significant differences are observed in the drag polar of small aircraft with low Reynolds numbers when compared to full-scale aircraft due to the high C_{D_0} and the effect of the propeller slipstream.

In order to facilitate the process of estimating the coefficient of parasite drag, approximate values can be established for each aircraft component which incorporate the average coefficients of friction, form factors, and, if applicable, slipstream dynamic pressures for all aircraft in the database. Each of these values is made independent of aircraft size, which makes using the values relatively easy. The values can be used to determine the total parasite drag coefficient according to

$$C_{D_P} \approx \frac{1}{S_{Ref}} \sum C_{D_\Pi} A_\Pi \qquad (5.1)$$

where S_{Ref} is still the wing area, C_{D_Π} is the equivalent parasite drag coefficient, and A_Π is the equivalent parasite area. The values of C_{D_Π} are approximated from the aircraft database. The values for the component drag coefficient values and areas can be obtained from Table 5.1—these values reflect the average values from the aircraft database. The table only includes values for the fuselage, wing, and tail assembly. Wheel struts and tires are not included because their component drag values are best approximated using a parasite drag coefficient value of 1.2. This is the standard parasite drag coefficient value for cylinders. Additionally, Appendix B includes a full listing of the C_{D_Π} values for each aircraft component from each aircraft in the database. The values in Appendix B were calculated using a free stream velocity of 15 m/s, a standard cruising velocity for electric-powered radio-controlled aircraft. For reference, the standard equivalent parasite drag coefficient values for full-scale, high Reynolds-number aircraft are displayed in Table 5.2. The equivalent parasite drag coefficient value is the same for small and large aircraft, indicating that the parasite drag of a wing is independent of wing size and Reynolds number. The equivalent drag values for the fuselage and tail sections, however, are much greater for low Reynolds number aircraft. This is primarily due to the effect of the slipstream dynamic pressure,

Table 5.1: Component Drag Coefficient Values for Low Reynolds Number Aircraft.

Component	$C_{D_{\Pi}}$	A_{Π}
Wing	0.00698	S_{Ref}
Fuselage	0.214	Fuselage Cross Section
Tail Assembly	0.0263	Horizontal Stabilizer Planform

Table 5.2: Component Drag Coefficient Values for Full-Scale Propeller Aircraft.[1]

Component	$C_{D_{\Pi}}$	A_{Π}
Wing	0.0070	S_{Ref}
Fuselage	0.1100	Fuselage Cross Section
Tail Assembly	0.0080	Horizontal Stabilizer Planform

which is especially important to consider on small aircraft, and the poor aerodynamic characteristics which are usually exhibited by radio-controlled aircraft.

A listing of the parasite coefficients of drag (by aircraft component) for each aircraft in the database is also included in Appendix D. Unlike the values in Appendix C, those in Appendix D are total values—they are not relative to the size of the aircraft component. These values are related to the total coefficient of parasite drag by the relation

$$C_{D_P} = Q \sum C_D \qquad (5.2)$$

where C_D is the drag coefficient value for each aircraft component. As Equation 5.2 indicates, a drag interference factor has not yet been applied to the values in Appendix C.

After analyzing each aircraft individually, trends were sought which related the data for all aircraft. Recognizing general trends in the drag and performance data is a useful method of predicting the aerodynamic characteristics of new aircraft designs. First, Figure 5.7 displays the ratio of fuselage length to fuselage diameter to the horizontal volume ratio. While the plot does not show strong correlation between the data points, there is a general trend of an increasing

---

[1] Roskam, Jan. "Methods for Estimating Drag Polars of Subsonic Airplanes. University of Kansas, 1971. Print.

volume ratio as the fuselage dimension ratio increases. Figure 5.8 plots wing loading versus aspect ratio. The aspect ratio is relatively constant as wing loading varies; however, there is a slight trend toward higher aspect ratios in aircraft with greater wing loadings. Figure 5.9 displays the thrust to weight ratio plotted against the maximum aircraft velocity. No strong trend emerges from this graph. Finally, Figure 5.10 is a plot of wing loading versus maximum velocity. While the data is fairly scattered, there is a general trend toward higher maximum velocities in aircraft with greater wing loadings.
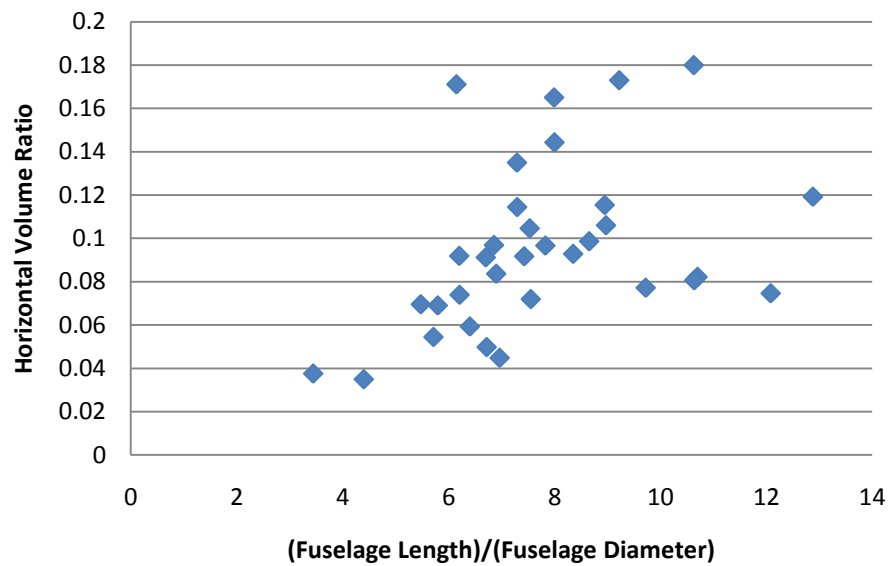

Figure 5.7: Fuselage Length to Diameter Ratio verses Horizontal Volume Ratio for all Test Aircraft.
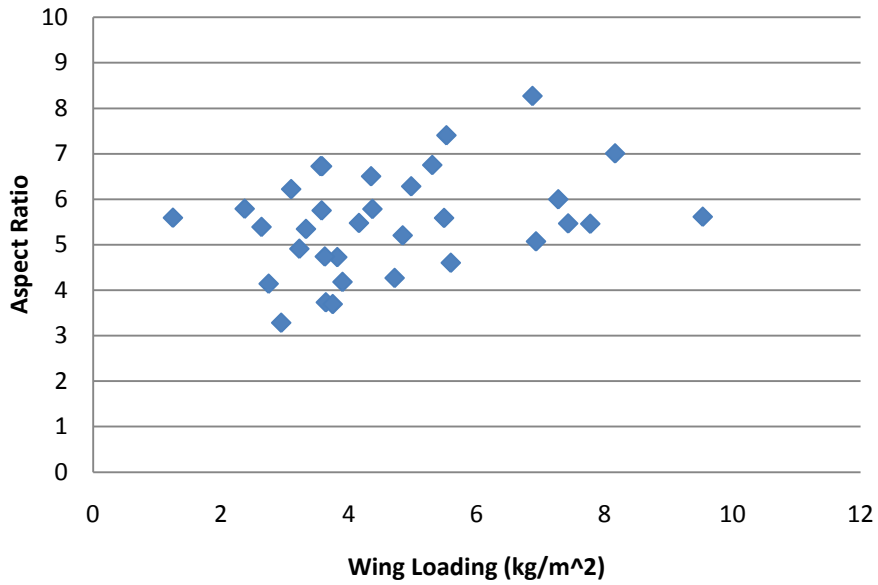
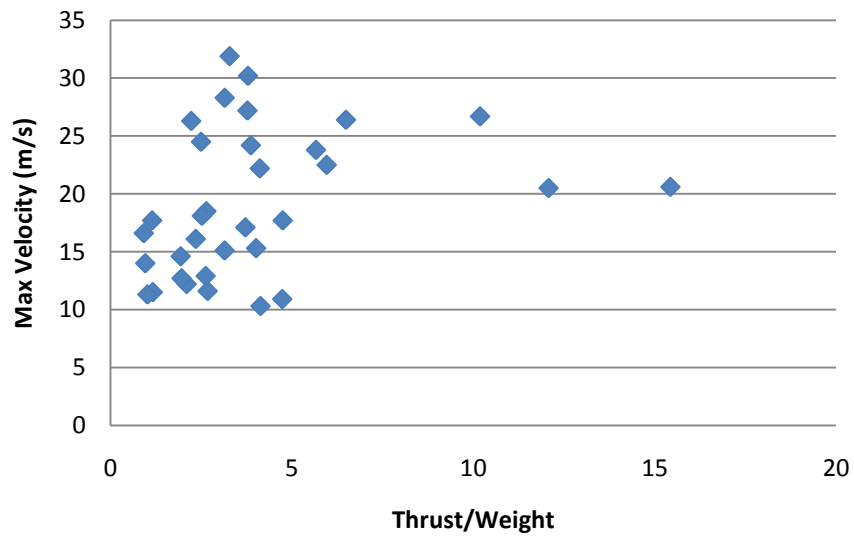**Figure 5.8:** Wing Loading verses Aspect Ratio for all Test Aircraft.

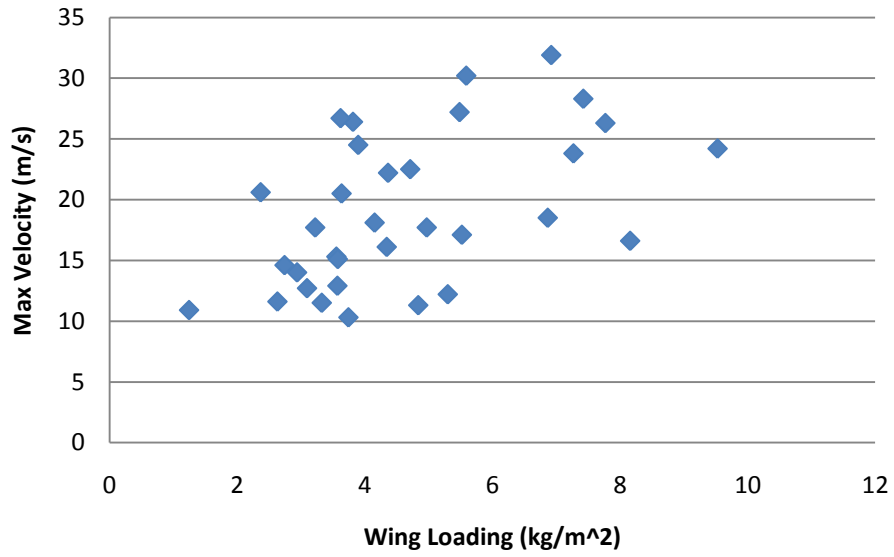**Figure 5.9:** Thrust to Weight Ratio verses Maximum Velocity for all Test Aircraft.

Figure 5.10: Wing Loading verses Maximum Velocity for all Test Aircraft.

Section 6

Conclusion

Because of the unique aerodynamic properties associated with small RPV and radio-controlled aircraft, they must be analyzed separately from full-scale aircraft. While the equations and relationships developed for large aircraft are applicable to small aircraft, they must be specially tailored to incorporate the large drag coefficients of small aircraft. By developing the power plant, propeller, drag, and performance theory as it applies to small aircraft, and then applying that theory to a database of radio-controlled aircraft, the unique behavior of small aircraft has been expounded. The basis of the aerodynamic analysis of low Reynolds number aircraft is the large drag which is experienced by small aircraft. To account for this, the dynamic pressure in the propeller's slipstream should be increased to compensate for the increase in the flow velocity. This is important for small aircraft because of the relatively large size of their motors and propellers compared to the airframe sizes. When this effect is considered, the parasite drag increases substantially, which has repercussions on aircraft performance. The aircraft require more power to maintain level, constant-velocity flight, and their maximum flying velocities are decreased. When applied to drag polar plots, compensating for the slipstream dynamic pressure increases the coefficient of drag as the coefficient of lift increases, and tends to make the drag polar plot relatively linear in shape.

Throughout this analysis, the equations and concepts have been explained, and were then applied to a database of aircraft. This fulfills the initial intent of using precedent data to synthesize information which can be applied to aid in designing a new aircraft. The information presented by the aircraft database serves as an initial reference in the design of new aircraft. The methods which were used to analyze each sample aircraft can be applied to the new aircraft design in order to study its aerodynamic and performance specifications. By focusing specifically on low Reynolds number aircraft, the methods and data presented in this analysis provide an effective basis for the preliminary design of low Reynolds number aircraft.

Appendix A

Matlab Code

Primary Program, rcairplane.m:

```matlab
%PERFORMANCE ANALYSIS OF LOW REYNOLDS NUMBER AIRCRAFT
%DANIEL L. SHAFFER & MICHAEL S. TURNER

%University of Notre Dame
%Department of Aerospace and Mechanical Engineering
%April 2010

%rcairplane.m
%Use this program in conjunction with the Excel files RC_specs.xls and
%RC_motor.xls and in conjunction with the functions Powerplant.m,
%PowerRequired.m, and AeroGraph.m.

close all
clear all

%Read in the Excel files containing the aircraft and motor specifications.
%Note: New aircraft and motors can easily be added by modifying the Excel
%source files.  However, the data range which Matlab reads must also be
%edited.

specs = xlsread('RC_Specs.xls','D7:S39');
motor = xlsread('RC_Motor','C7:I26');

[num_planes,width] = size(specs);

%Prompt the user to input which model to analyze
row_plane = input('Input the number which corresponds to the aircraft which
you would like to analyze: ');
while row_plane > num_planes || row_plane < 0
    row_plane = input('Invalid aircraft number. Input the number which
corresponds to the aircraft which you would like to analyze: ');
end

[num_motors,motor_width] = size(motor);

motor_num=specs(row_plane,9);
for row = 1:num_motors
    if motor_num == motor(row,1)
        row_motor = row;
        break
    end
end
```

```matlab
%Display a message that identifies the aircraft analysis results:
display('Aircraft Analysis Results:')

%Run a function to complete the power plant and propeller analysis.
[pow_av prop_thrust] = Powerplant(motor(row_motor,:),specs(row_plane,:));

%Run a function to comlete the drag analysis.
[vel pow_req Cl Cd P_par P_ind] =
PowerRequired4(specs(row_plane,:),prop_thrust);

%Run a function to create the plots.
AeroGraph(vel,pow_req,Cl,Cd,pow_av,P_par,P_ind);
```

Function, Powerplant.m:

```matlab
%PERFORMANCE ANALYSIS OF LOW REYNOLDS NUMBER AIRCRAFT

%DANIEL L. SHAFFER & MICHAEL S. TURNER

%University of Notre Dame
%Department of Aerospace and Mechanical Engineering
%April 2010

%Powerplant.m
%This function analyzes the aircraft's motor and propeller in order to
%determine the power available.  Additionally, the program outputs useful
%parameters including propeller efficiency and the thrust produced.

function [Pav thrust] = Powerplant(motor, specs)

%Assign a name to each applicable variable which was imported.
voltage = motor(3);
KV = motor(4);
current = motor(5);
prop_dia = specs(7)/12; %In feet
prop_pitch = specs(8)/12; %In feet
P_motor = motor(6); %Motor Power, if supplied by manufacturer
rpm = motor(7); %Maximum RPM, if supplied by manufacturer
rho = 0.002378; %Air density, in slug/ft^3

%Propeller pitch to diameter ratio:
prop_ratio = prop_pitch/prop_dia;

%Calculate power produced by motor, if not specified by manufacturer:
if P_motor == 0
    P_motor = voltage*current;
end

%Estimate the motor efficiency based upon the motor's power:
```

46

```matlab
motor_eff = -1.621e-7*P_motor^2 + 0.0003732*P_motor + 0.7066;

%Apply the efficiency factor to find the output power:
if P_motor <= 1200
    P_out = motor_eff*P_motor;
elseif P_motor > 1200
    P_out = 0.9*P_motor;
end

%Convert to horsepower:
P_motorhp = P_out/745.7;

%Calculate maximum RPM, if not specified by manufacturer:
if rpm ==0
    rpm = KV*voltage;
end

%Coefficient of Power (Includes conversion to horsepower):
Cp = P_motorhp*550/(rho*(rpm/60)^3*(prop_dia)^5);

%Calculate advance ratio (J) from Cp:
if prop_ratio <= 0.45
    %Equation valid for 0.3<J<0.8
    J = -3.949e4*Cp^3 + 957.1*Cp^2 - 16.35*Cp + 0.8004;
elseif prop_ratio > 0.45 && prop_ratio <= 0.55
    %Equation valid for 0.3<J<0.9
    J = -516*Cp^2 + 1.058*Cp + 0.885;
elseif prop_ratio > 0.55 && prop_ratio <= 0.65
    %Equation valid for 0.4<J<1.0
    J = -1.477e4*Cp^3 + 566.4*Cp^2 - 13.97*Cp + 1.002;
elseif prop_ratio > 0.65 && prop_ratio <= 0.75;
    %Equation valid for 0.4<J<1.1
    J = -8220*Cp^3 + 336.7*Cp^2 - 10.93*Cp + 1.103;
elseif prop_ratio > 0.75 && prop_ratio <= 0.85
    %Equation valid for 0.5<J<1.3
    J = -7995*Cp^3 + 533.6*Cp^2 - 18.78*Cp + 1.288;
elseif prop_ratio > 0.85
    %Equation valid for 0.5<J<1.4
    J = -5185*Cp^3 + 396.2*Cp^2 - 16.95*Cp + 1.405;
end

%Velocity of air flowing through propeller:
vel = J*(rpm/60)*prop_dia;

%Calculate Coefficient of Thrust:
if prop_ratio <= 0.45
    Ct = -0.1225*J + 0.0965;
elseif prop_ratio > 0.45 && prop_ratio <= 0.55
    Ct = -0.1185*J + 0.106;
elseif prop_ratio > 0.55 && prop_ratio <= 0.65
    Ct = -0.123*J + 0.1218;
elseif prop_ratio > 0.65 && prop_ratio <= 0.75
    Ct = 0.07755*J^3- 0.1569*J^2 - 0.02159*J + 0.1132;
elseif prop_ratio > 0.75 && prop_ratio <= 0.85
    Ct = 0.06944*J^3 - 0.1714*J^2 + 0.01163*J + 0.1133;
```

```matlab
elseif prop_ratio >0.85
    Ct = 0.06944*J^3 - 0.1795*J^2 + 0.03306*J + 0.1131;
end

%Propeller Thrust (in pounds)force:
thrust_lb = Ct*rho*(rpm/60)^2*prop_dia^4;

%Convert thrust to Newtons:
thrust = thrust_lb*4.4482;
display(['Total Thrust: ' num2str(thrust) ' N']);

%Propeller Efficiency:
prop_eff = Ct*J/Cp;
eff_perc = prop_eff*100;
display(['Propeller Efficiency: ' num2str(eff_perc) ' %']);

%Power Available:
Pav = P_out*prop_eff;
display(['Power Available: ' num2str(Pav) ' W']);

end
```

Function, PowerRequired4.m:

```matlab
%PERFORMANCE ANALYSIS OF LOW REYNOLDS NUMBER AIRCRAFT

%DANIEL L. SHAFFER & MICHAEL S. TURNER

%University of Notre Dame
%Department of Aerospace and Mechanical Engineering
%April 2010

%PowerRequired4.m
%This function completes the drag analysis for a given airplane and outputs
%the range of flying velocities and the associated drag values.

function [vel P Cl_wing Cd_total P_p P_i] = PowerRequired4(specs,thrust)

%Assign a name to each variable which was imported.
fus_length = specs(2);
wingspan = specs(3);
wing_area = specs(4);
weight = specs(6);
prop_dia = specs(7)*0.0254;%Convert propeller dimeter to meters
fus_dia = specs(10);
strut_l = specs(11);
no_tires = specs(12);
h_tail_area = specs(13);
v_tail_area = specs(14);
tailspan = specs(15);
```

```matlab
tire_dia = specs(16);


%Establish the value which are needed for drag calculations and which
%remain constant with time.
rho = 1.225; %Air Density
mu = 1.789e-5; %Air Viscosity
wing_chord = wing_area/wingspan; %Wing Chord Length
tail_chord = h_tail_area/tailspan; %Tail Chord Length
S_ref = wing_area; %Reference Area
FR = fus_length/fus_dia; %Fineness Ratio
K_f = 1 + 60/FR^3 + FR/400; %Fuselage form Factor
Swet_wing = wing_area*2*1.02; %Wetted Wing Area
Swet_fus = pi*fus_dia*fus_length*(1 - 2/FR)^(2/3)*(1 + 1/FR^2); %Wetted
Fuselage Area
Swet_tail = (h_tail_area + v_tail_area)*2*1.02; %Wetted Tail Area
Swet_strut = strut_l*0.0149606;  %Standard Cross-Sectional Area of Strut
Wire, assuming 3/16 inch diameter wire
tire_width = 0.0127; %Standard Width of Tire;
Swet_tire = (2*(pi/4)*tire_dia^2) + (tire_width*pi*tire_dia); %Wetted Tire
Area
AR = wingspan^2/wing_area; %Wing Aspect Ratio
fus_xsec = (pi/4)*fus_dia^2; %Fuselage Cross-Sectional Area
Z = 2; %Sweep correction factor at low Mach numbers with no wing sweep
t_c = 0.1; %Wing chord length to thickness ratio
K_w = 1 + Z*(t_c) + (t_c)^4; %Wing form factor


%Set the range of velocities over which the analysis will be conducted.
vmin = 0.1;
vmax = 100;


%Create an array with the velocities which correspond to the drag analysis.
vel=vmin:0.1:vmax;


%Calculate the induced drag coefficient:
e_wing = 0.0008*AR^3 - 0.02*AR^2 + 0.14*AR + 0.56;
oswald_fus = 0.002414*AR^2 + 0.06075*AR + 1.228;
e_fus = oswald_fus*fus_xsec/S_ref;
e_tot = 1/((1/e_wing) + (e_fus) + 0.05);
k = 1/(pi*AR*e_tot);


%Establsih the loop which will calculate drag at each velocity.
i = 0;
num_entries = length(vel);
P = zeros(num_entries,1);
Re_wing = zeros(num_entries,1);
Re_fus = zeros(num_entries,1);
Re_tail = zeros(num_entries,1);
Cf_wing = zeros(num_entries,1);
Cf_fus = zeros(num_entries,1);
Cf_tail = zeros(num_entries,1);
qinf = zeros(num_entries,1);
qinf_vtx = zeros(num_entries,1);
Cd_fus = zeros(num_entries,1);
Cd_wing = zeros(num_entries,1);
Cd_tail = zeros(num_entries,1);
Cd_strut = zeros(num_entries,1);
```

```matlab
Cd_tire = zeros(num_entries,1);
Cd_p_tot = zeros(num_entries,1);
Cl_wing = zeros(num_entries,1);
Cl_wing2 = zeros(num_entries,1);
Cd_i_tot = zeros(num_entries,1);
Cd_total = zeros(num_entries,1);
P_p = zeros(num_entries,1);
P_i = zeros(num_entries,1);


for v = vmin:0.1:vmax

    i = i + 1;


    %Reynolds Number for each aircraft component:
    Re_wing(i) = rho*v*wing_chord/mu;
    Re_fus(i) = rho*v*fus_length/mu;
    Re_tail(i) = rho*v*tail_chord/mu;
    %Skin Friction Coefficient for each aircraft component:
    Cf_wing(i) = 0.455/(log10(Re_wing(i)))^2.58;
    Cf_fus(i) = 0.455/(log10(Re_fus(i)))^2.58;
    Cf_tail(i) = 0.455/(log10(Re_fus(i)))^2.58;
    %Dynamic Pressure:
    qinf(i) = 0.5*rho*v^2;
    %Dynamic Pressure in Slipstream:
    qinf_vtx(i) = 0.5*rho*v^2 + thrust/((pi/4)*prop_dia^2);


    %Calculate the parasitic drag for each aircraft component:
    Cd_fus(i) = (K_f*Cf_fus(i)*Swet_fus*qinf_vtx(i))/(S_ref*qinf(i));
    Cd_wing(i) = (K_w*Cf_wing(i)*Swet_wing)/S_ref;
    Cd_tail(i) = (K_w*Cf_tail(i)*Swet_tail*qinf_vtx(i))/(S_ref*qinf(i));
    Cd_strut(i) = (1.2*Swet_strut*qinf_vtx(i))/(S_ref*qinf(i));
    Cd_tire(i) = (1.2*Swet_tire*qinf_vtx(i))/(S_ref*qinf(i));


    %Total Parasite Drag Coefficient:
    Cd_p_tot(i) = 1.2*(Cd_fus(i) + Cd_wing(i) + Cd_tail(i) + Cd_strut(i) +
no_tires*Cd_tire(i));


    %Coefficient of Lift:
    Cl_wing(i) = (weight*9.81)/(qinf(i)*wing_area);
    %Coefficient of Lift Squared for Drag Polar:
    Cl_wing2(i) = (Cl_wing(i))^2;


    %Total Induced Drag Coefficient:
    Cd_i_tot(i) = k*(Cl_wing(i))^2;


    %Total Drag Coefficient:
    Cd_total(i) = Cd_p_tot(i) + Cd_i_tot(i);


    %Power Required:
    %Due to Parasite Drag:
    P_p(i) = 0.5*rho*wing_area*v^3*Cd_p_tot(i);
    %Due to Induced Drag:
    P_i(i) = 0.5*rho*wing_area*v^3*Cd_i_tot(i);
    %Total:
    P(i) = P_p(i) + P_i(i);
```

```matlab
end
end
```

Function, AeroGraph.m:

```matlab
%PERFORMANCE ANALYSIS OF LOW REYNOLDS NUMBER AIRCRAFT

%DANIEL L. SHAFFER & MICHAEL S. TURNER

%University of Notre Dame
%Department of Aerospace and Mechanical Engineering
%April 2010

%AeroGraph.m
%The function produces two plots to display the analysis results.  The
%first plot shows power required and power available with increasing
%velocity.  The second plot is a drag polar,  which compares the
%coefficient of lift and the coefficient of drag.

function AeroGraph(v, Preq, Cl_wing, Cd_total, Pav,P_p,P_i)

%Create the power available and power required plot.
figure('Name','Power','NumberTitle','off')
plot(v,Preq,'k')
v_last = length(v);
hold on
dragx = [v(1); v(v_last)];
dragy = [Pav; Pav];
plot(dragx,dragy,'r')
plot(v,P_p,'g:')
plot(v,P_i,'b:')

%Find the maximum x value for the plot axis (using the fact that the step
%size from the Power required function is 0.1:
for iteration = 2:length(Preq)
    %Calculate the point in the Preq matrix where the lowest value occurs:
    if Preq(iteration) > Preq(iteration-1)
        xstart = iteration;
        minP = Preq(iteration);
        display(['Minimum Power Required: ' num2str(minP) ' W']);
        break
    end
end
for xpoint = xstart:length(v)
    %Determine where the Power Required and Power Available Lines intersect:
    if Preq(xpoint) >= Pav
        %Set the maximum x axis value to be 5 m/s greater than the
        %intersection point:
        xmax = xpoint/10 + 5;
        v_hi = v(xpoint);
        display(['Maximum Velocity: ' num2str(v_hi) ' m/s']);
```

```matlab
        break
    end
end
axis([0 xmax 0 Pav+0.4*Pav])

xlabel('Velocity [m/s]')
ylabel('Power [W]')
title('Power Required and Available vs. Velocity','FontWeight','b')
legend('Power Required','Power Available','Parasite Component','Induced
Component','Location','best')

%Create the drag polar plot.
figure('Name','Drag Polar','NumberTitle','off')
plot(Cl_wing,Cd_total)
ymin=Cd_total(length(Cd_total))-0.1;
if ymin < 0
    ymin = 0;
end

for ypoint = 1:length(Cl_wing)
    if Cl_wing(ypoint) <= 1.5
        y_axismax = Cd_total(ypoint) + 0.05;
        break
    end
end

axis([0 1.5 ymin y_axismax])
xlabel('Coefficient of Lift')
ylabel('Coefficient of Drag')
title('Drag Polar: Coefficient of Lift vs. Coefficient of
Drag','FontWeight','b')

end
```

Appendix B

Data for Equivalent Drag Coefficient Calculation

Equivalent drag coefficient value for the fuselage, wing, and tail assembly for each database aircraft, listed by aircraft reference number:

Aircraft Reference Number	Fuselage	Wing	Tail
1	0.2514	0.0074	0.0328
2	0.1974	0.0075	0.0220
3	0.3266	0.0065	0.0446
4	0.2771	0.0071	0.0307
5	0.2151	0.0068	0.0173
6	0.2399	0.0069	0.0278
7	0.1953	0.0063	0.0235
8	0.1501	0.0072	0.0245
9	0.2317	0.0066	0.0212
10	0.1475	0.0073	0.0192
11	0.2697	0.0066	0.0365
12	0.4802	0.0065	0.0439
13	0.2529	0.0070	0.0189
14	0.4482	0.0067	0.0359
15	0.1457	0.0060	0.0199
16	0.1300	0.0064	0.0181
17	0.1511	0.0075	0.0218
18	0.1779	0.0072	0.0248
19	0.1471	0.0064	0.0261
20	0.1651	0.0068	0.0291
21	0.2091	0.0069	0.0309

22	0.1607	0.0075	0.0204
23	0.2713	0.0068	0.0354
24	0.1263	0.0070	0.0186
25	0.1728	0.0075	0.0222
26	0.1537	0.0073	0.0266
27	0.1804	0.0072	0.0281
28	0.1475	0.0069	0.0187
29	0.2210	0.0074	0.0221
30	0.2292	0.0071	0.0265
31	0.1466	0.0074	0.0226
32	0.1376	0.0073	0.0219
33	0.3083	0.0073	0.0345
Average	0.2141	0.0070	0.0263
Std. Dev.	0.0842	0.0004	0.0072

Appendix B

Data for Parasite Drag Coefficients

The total drag parasite drag coefficient for each database aircraft, listed by aircraft reference number:

Aircraft Reference Number	Fuselage	Wing	Tail	Landing Gear Strut	Tire
1	0.0185	0.0151	0.0055	0.0513	0.0586
2	0.0111	0.0153	0.0066	0.0582	0.0387
3	0.0112	0.0132	0.0090	0.1481	0.0231
4	0.0118	0.0114	0.0077	0.0340	0.0255
5	0.0050	0.0138	0.0029	0.0116	0.0105
6	0.0117	0.0142	0.0046	0.0315	0.0129
7	0.0068	0.0128	0.0071	0.0124	0.0161
8	0.0133	0.0147	0.0068	0.0258	0.0258
9	0.0065	0.0135	0.0058	0.0139	0.0104
10	0.0076	0.0150	0.0048	0.0289	0.0131
11	0.0118	0.0135	0.0037	0.2021	0.0121
12	0.0089	0.0133	0.0063	0.0745	0.0143
13	0.0045	0.0142	0.0032	0.0365	0.0181
14	0.0090	0.0136	0.0040	0.0414	0.0171
15	0.0064	0.0122	0.0040	0.0353	0.0629
16	0.0088	0.0130	0.0018	0.0073	0.0078
17	0.0091	0.0153	0.0027	0.0303	0.0149
18	0.0165	0.0148	0.0035	0.0340	0.0142
19	0.0101	0.0131	0.0034	0.0444	0.0063
20	0.0325	0.0138	0.0049	0.0222	0.0038
21	0.0140	0.0141	0.0044	0.0234	0.0158

22	0.0068	0.0154	0.0029	0.0810	0.0455
23	0.0139	0.0139	0.0071	0.0298	0.0203
24	0.0092	0.0144	0.0031	0.0163	0.0324
25	0.0113	0.0153	0.0037	0.0497	0.0147
26	0.0204	0.0148	0.0022	0.0824	0.0208
27	0.0105	0.0148	0.0040	0.1425	0.0229
28	0.0075	0.0141	0.0031	0.0284	0.0097
29	0.0066	0.0150	0.0032	0.0329	0.0151
30	0.0101	0.0144	0.0044	0.0334	0.0237
31	0.0117	0.0151	0.0032	0.0289	0.0134
32	0.0127	0.0149	0.0029	0.0650	0.0253
33	0.0142	0.0148	0.0053	0.0379	0.0246
Average	0.0112	0.0141	0.0045	0.0483	0.0209
Std. Dev.	0.005285	0.000971	0.001744	0.042416	0.013558

Bibliography

All specifications and dimensions for the aircraft database were obtained from the manufacturers' websites. The manufacturer of each aircraft and motor is listed in the database. All data can be accessed from these websites.

Anderson, John David. *Introduction to Flight*. Boston: McGraw-Hill, 2008. Print.

Hoerner, Sighard F. *Fluid-Dynamic Drag*. Brick Town: Hoerner Fluid Dynamics, 1965. Print.

Lennon, Andy. *RC Model Airplane Design*. Osceola, Wis., USA: Motor International, 1986.
     Print.

Roskam, Jan. *Airplane Design*. Ottawa: Roskam Aviation and Engineering Corporation, 1985.
     Print.

Roskam, Jan. "Methods for Estimating Drag Polars of Subsonic Airplanes. University of
     Kansas, 1971. Print.